

Verifying the BR-DTS method with hand measurements executed with the PT-100 and the Eddy Covariance method

T.A. v. Iersel, A. M. J. Coenders-Gerrits, B. Schilperoort

Delft University of Technology, Water Resources Section, Stevinweg 1, 2628 CN Delft, the Netherlands
16 December 2016

Abstract

Within hydrology evaporation is one of the most important terms in the water- and land surface energy balance. However evaporation is difficult to estimate accurately. Conventional techniques to measure actual evaporation have their drawbacks. One of the main drawbacks is that multiple sensors need to be used, with all their own bias. One of these techniques, the Eddy Covariance (EC) system has the drawback that it is dependent on weather conditions and is known for its problems with closure of the energy balance (Foken, 2008). A new method called the Bowen Ratio- Distributed Temperature Sensing (BR-DTS) method is introduced by Euser et al. (2014). This method determines the Bowen ratio which is the ratio between the sensible heat flux and the latent heat flux. The BR-DTS method measures temperature using a fiber optic cable. This cable is placed vertically along a tower, the cable going up is dry and the cable going down is wrapped in cotton and kept wet. With the dry and wet temperature of the DTS-cable the air temperature and vapour pressure can be determined. By having a large amount of measurements over the height and measuring it with a single sensor the BR-DTS method does not have the problem of varying biases of sensors (Euser et al. 2014). The aim of this study is at first to verify if the temperature data of the dry and wet cable are correct and second to compare the outcome with the EC data. The temperature of the dry and wet cable measured with the BR-DTS method are really close to the temperatures measured with the relative humidity sensors with a maximum R^2 of 0.998 at 4 and 16 meter height for the dry cable and a maximum R^2 of 0.988 at 16 meter height for the wet cable. The energy gap found is relatively small, see figure 11, and the latent heat flux measured with the BR-DTS setup is just as in the results from B. Schilperoort (2015) greater than the latent heat flux measured with the EC setup. On the other hand the sensible heat flux measured with the BR-DTS setup is smaller than the sensible heat flux measured with the EC setup which is in contradiction with the results from B. Schilperoort (2015).

1 Introduction

Within hydrology, evaporation is one of the most important terms in the water balance and the land surface energy balance. The water balance equation describes the water fluxes in and out of a closed system using the principles of conservation of mass. All precipitation entering the system must be transferred into either evaporation, run off or stored in the ground.

In a land surface energy balance, the net radiation is partitioned in heating the air (sensible heat), heating the ground (ground heat flux) and in evaporating water (latent heat). Latent heat ($W m^{-2}$) is the product of the evaporation ($mm s^{-1}$), latent heat of vaporization ($2.45 MJ kg^{-1} K^{-1}$) and density of water (kg/m^3). The latent heat flux is the energy absorbed by or released from a substance during a phase change from a gas to a liquid or a solid or vice versa. Accurate values for actual evaporation are needed for hydrological, environmental and irrigation studies and are become more important with the problems of climate change. However evaporation is difficult to estimate accurately. Conventional techniques to measure actual evaporation have their drawbacks. One of the main drawbacks is that multiple sensors have to be used, with all their own bias. One of these techniques, the Eddy Covariance system has as a drawback that it is dependent on weather conditions. The Eddy Covariance system is not reliable during rain or lack of wind and is known for its problems with closure of the energy balance (Foken, 2008).

A new method called the Bowen Ratio-DTS (BR-DTS) method is introduced by Euser et al. (2014). This method determines the Bowen ratio which is the ratio between the sensible heat flux and the latent heat flux, and uses the air temperature gradient and the vapour pressure gradient over the height (Bowen, 1926). The BR-DTS method measures temperature using a fiber optic cable. This cable is placed vertically along a tower, the cable going up is dry and the cable going down is wrapped in cotton and kept wet with a pump on top of the tower. With the dry and wet temperature of the distributed temperature sensing-cable (DTS-cable) the air temperature and vapour pressure can be determined.

By having a large amount of measurements over the height and measuring it with a single sensor the

BR-DTS methods does not have the problem of varying biases or sensors (Euser et al. 2014).

The aim of this study is first to verify if the temperature data of the dry and wet cable are correct and second to compare the outcome with the Eddy Covariance (EC) data. The measurements were performed in summer of 2016 in the Netherlands.

2 Materials and methods

2.1 Study area

The measurements for this study were carried out in a forest called Speuldersbos. This forest is located near the village of Garderen in the Netherlands. The forest is a mixture between pine trees consisting of larch, Scott's Pine, Douglas fir, and broadleaves beech. In a patch of Douglas fir a measurement tower of 48 meter height is situated. The height of the trees vary between 26 and 38 meter. The yearly average temperature in the area is 9.8 °C, an average precipitation of 910 mm/year and prevailing south-west wind (KNMI, 2011). The closest KNMI measurement station is 30 km away from the tower in the village of Deelen. The measurements were carried out from the 3rd of August till the 23rd of August in 2016.

2.2 BR-DTS method

2.2.1 BR-DTS theory

As previously mentioned will this study be using the BR-DTS method. The Bowen ratio can be determined with the actual air temperature and the actual vapour pressure over a vertical air column (Bowen, 1926). However to use the BR method some assumptions need to be made (Angus and Watts, 1984; Fritschen and Simpson, 1989; Gavilán: and Berengena, 2007; Spittlehouse and Black, 1980):

- Fluxes are only one dimensional without a horizontal gradient.
- Measurement sensors are located in the equilibrium sub-layer where fluxes are constant with height.
- Land surface is homogenous with respect to sources and sinks of heat, water vapour and momentum.
- Turbulent exchange coefficients for heat and vapour fluxes are assumed to be equal.

The Bowen ratio, β , can be determined by dividing the sensible heat flux, H (W m^{-2}), through the latent heat flux, $\rho\lambda E$ (W m^{-2}). The β is also equal to the ratio between ΔT_a and Δe_a times γ .

$$\beta = \frac{H}{\rho\lambda E} = \gamma \frac{\Delta T_a}{\Delta e_a} \quad (1)$$

Where γ is the psychrometric constant ($\text{kPa } ^\circ\text{C}^{-1}$), T_a is the air temperature ($^\circ\text{C}$) and e_a is the actual vapour pressure (kPa). Based on the dry and wet bulb measurements the actual vapour pressure can be determined with Eq. (2) (Allen et al., 1998).

$$e_a = e_s - \gamma(T_a - T_w) \quad (2)$$

Where T_w is the temperature of a wetted and well ventilated surface alias wet bulb temperature ($^\circ\text{C}$), e_s is the saturated vapour pressure (kPa). The saturated vapour pressure can be determined with Eq. (3) (Bohren and Albrecht, 1998).

$$e_s = 0.61e^{\frac{19.9 T_w}{273+T_w}} \quad (3)$$

The psychrometric constant is, in case of a sufficiently ventilated psychrometer, defined as following (Allen et al. 1998):

$$\gamma = \frac{c_p P}{\varepsilon \lambda} \cong 0.665 * 10^{-3} P \quad (4)$$

Where c_p is the specific heat of air ($1.013 \text{ KJ kg}^{-1} \text{ K}^{-1}$), P is the atmospheric pressure (kPa), λ is the latent heat of vaporization ($2.45 \text{ MJ Kg}^{-1} \text{ K}^{-1}$) and ε is the ratio between molecular masses of water vapour and dry air (Allen et al. 1998).

When Eqs. (1), (2) and (3) are combined over a vertical air column the Bowen ratio can be calculated with just γ and T_a and T_w over multiple heights (Eq. 5).

$$\beta = \gamma \frac{\Delta T_a}{\Delta(0.61e^{\frac{19.9 T_w}{273+T_w}}) - \gamma\Delta T_a + \gamma\Delta T_w} \quad (5)$$

The Bowen ratio can be combined with measurements for R_n and G to calculate the latent heat flux (Eq.6) and the sensible heat flux (Eq. 7) (Aston, 1985; Fritschen, 1965; Perez et al., 1999). Where R_n is the net radiation (W m^{-2}) and G the storage term of the energy balance (W m^{-2}). Because the storage term of the energy balance is not measured it is assumed to be one percent of the net radiation.

$$\rho\lambda E = \frac{R_n - G}{1 + \beta} \quad (6)$$

$$H = \frac{\beta(R_n - G)}{1 + \beta} \quad (7)$$

2.2.2 BR-DTS set-up

The DTS technique measures the temperature distribution along a fibre optic cable with a diameter of 6 mm. The BR-DTS set-up makes use of the fibre optic cable and a computer, the Silixa Ultima, equipped with a laser transmitter and receiver. The fibre optic cable goes from the Ultima to the calibration bath up to the top of the tower at 48 meter, at a distance of 1.2 meter away from the tower (figure 1). At the top of the tower the cable is secured and goes down again, at a distance of 0.25 meter from the tower, to the calibration bath and Ultima again. This part of the cable is wrapped in cotton. The pump on top of the tower is constantly pumping water to the cable wrapped in cotton at a rate of 800 mL hr⁻¹. After the 23rd of August the rate is increased to 900 mL/hr due to the fact that it was noticed that on a warm day as the 23rd of August the wet cable was not wet over the entire height. The water supply is meant to keep the cable wet along the entire height of the tower, the excess water is recaptured at the bottom of the tower. In the calibration bath two PT100 probes are placed and connected to the Ultima. Next to the dry part of the 6 mm cable a cable with a diameter of 3 mm is situated which also measures the temperature. A sunscreen is placed between 36 and 46 m to put the cable, both wet and dry, in the shade. This is to reduce heating of the cable by solar radiation. Only the data between 36 and 46 m height of the tower is used to determine the Bowen ratio. The Ultima sends a laser pulse through the cable and analyzes the reflection. From the amplitude ratios between the reflected frequencies, the temperature can be derived (Selker et al., 2006). The Silixa Ultima uses a single end mode and a sampling resolution of 12.5 cm (Silixa, 2015) and measures every minute.

2.3 Reference techniques

The temperatures obtained with the DTS cable were compared to the temperatures given by the hand measurements with two PT100 probes and the temperatures measured by the humidity sensors. The latent and sensible heat fluxes obtained with the DTS method and the net radiation measurements were compared to the EC data. This chapter provides information about the PT100, humidity sensors, EC system and the net radiation gauge.

2.3.1 PT100

The PT100 consists of two RTD temperature probes and a precision thermometer from the brand Fluke, it is used to measure temperature. In this study it is used to compare to the temperatures found with the DTS technique. A set-up was made where one probe was wrapped with cotton and kept wet to simulate the wet part of the DTS cable, the other probe simulates the dry part of the DTS cable.

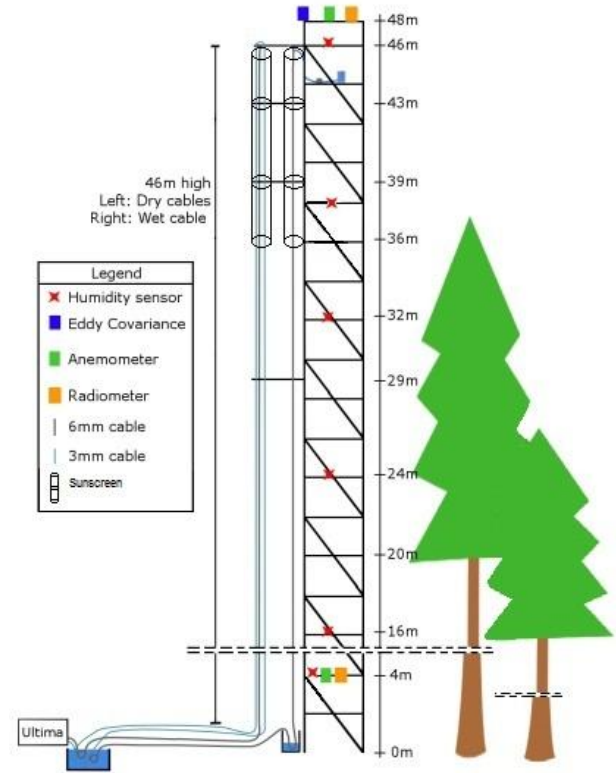


Figure 1 Schematic overview of the measurement tower with DTS set-up. Based on Schilperoord, 2015

Measurements were carried out at several heights in the tower at the 12th, 16th and 23rd of August. Both probes were ventilated during the measurements.

2.3.2 Humidity sensor

Six humidity sensors are located at the tower at several heights, in table 1 the characteristics per gauge are presented. The humidity sensors measure the relative humidity, ϕ (%), and the air temperature with which the wet bulb temperature can be obtained iterative. Combining Eq. (2) and (3) with Eq. (8) for the relative humidity (Maidment, 1993) enables to derive the wet bulb temperature.

$$\phi = \frac{e_a}{e_s} \quad (8)$$

Height	Brand	Model	Ventilated
4 m	Rotronic	HC2-S3C03	Yes
16 m	Rotronic	HC2-S3C03	Yes
24 m	Rotronic	HC2-S3C03	Yes
32 m	Rotronic	HC2-S3C03	Yes
38 m	Campbell	CS215	No
46 m	Campbell	CS215	No

Table 1 Humidity sensor information

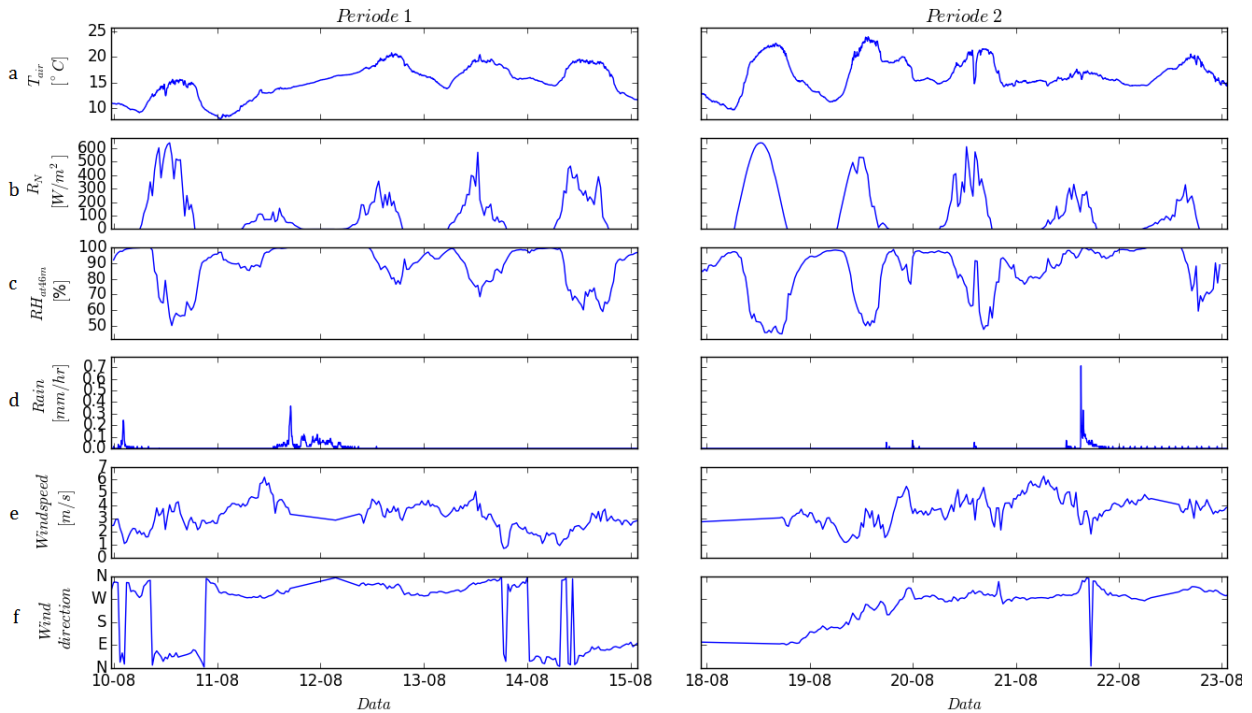


Figure 2 Meteorological conditions

2.3.3 Eddy covariance

The Eddy Covariance (EC) system measures the vertical transfer of water vapour driven by convection and senses the properties of eddies which determines the sensible and latent heat fluxes (Burba, 2013). On the tower the EC system, consisting of a Campbell CSAT3 sonic anemometer and a Li-Cor Biosciences L17500 gas analyser connected to a data logger, is installed at 48 m. In figure 1 another EC system at 35 m height is shown, this EC system was not working during the study period. The EC system is only reliable when the assumption can be made that there is no rain or lack of wind. In the timeframe of the 3rd of August till the 23rd of August in 2016 the EC system was not working on the 12th and between the 15th and the 18th of August.

2.3.4 Net radiation

The applications of the BR-DTS method makes use of measurements of the net radiation as shown in Eq. 6 and 7. The net radiometer at 44 m height measures both the incoming and outgoing short- and long wave radiation. The net radiometer used are Kipp & Zonen CNR4 net radiometers.

3 Results and Discussion

3.1 Meteorological conditions

In figure 2 the meteorological conditions of two periods are presented. Period one is from the 10th till the 15th of August and period two is from the 18th till the 23rd of August, these are the periods of which good EC data is available. Figure 2a shows the air temperature measured by the relative

humidity sensor, 2b shows the net radiation, 2c shows the relative humidity, 2d shows the throughfall measured with the Rain Gauge Data Logger model RG3-M and figure 2 e and f show the wind speed and direction measured with the EC system.

3.2 Temperature profile

In figure 3 and 4 the dry and wet temperature over the height of the tower on the 16th of August is shown. In appendix I the same figures for the 12th and the 23rd of August can be found, in this appendix the temperature measured with the thin cable is added and called 3mm up or 3mm down. At first it is important to notice that during daytime the wet cable is colder than the dry cable and during the night the temperature of the wet and dry cable approach each other. Secondly the effect of the screen, from 36 till 46 m, is clearly visible in both the temperature of the dry and wet DTS cable. Interesting is the effect of the floors of the tower, in the morning between 7am and 10am when the sun comes up from the east the sunlight is shining through the tower on to the cable. From this angle the cable is not shaded by the screen and so the shade caused by the floors of the tower is resulting in spatial temperature differences of the cable. In the canopy is the temperature of the dry cable higher than under or above the canopy. Under the canopy is the most shade and above the canopy the screen ensures shade in between 36-46 meters height. Just below the screen at 36 meter there is almost no shade because very few trees have a height larger than 36 meter. Going down from 36 m

height the canopy density becomes larger and the temperature of the dry cable decreases. The canopy density is largest around 25 meter height. For the temperature of the wet cable the same effect of shading is seen but here the effect of the wind speed is also important. Above the canopy is the largest wind speed which is essential for evaporation. In the canopy the wind speed is the lowest, the denser the canopy the lower the wind speed which results in a higher temperature of the wet cable. It is possible to conclude the effectiveness of the sun screen to be high (figure 3 and 4). The contrast of the temperature of the dry and wet cable just below and behind the sun screen is large. In all the figures in appendix I the same phenomenon can be found. The large contrast also shows that the sunscreen is too short. In between +/- 27 and 36 m the cables are not shaded by the screen and also not enough by the trees. The fact that in the morning, between 7am and 10am, the floors of the tower can clearly be seen makes it possible to conclude that the screen is not installed at the most efficient position in reference to the cable.

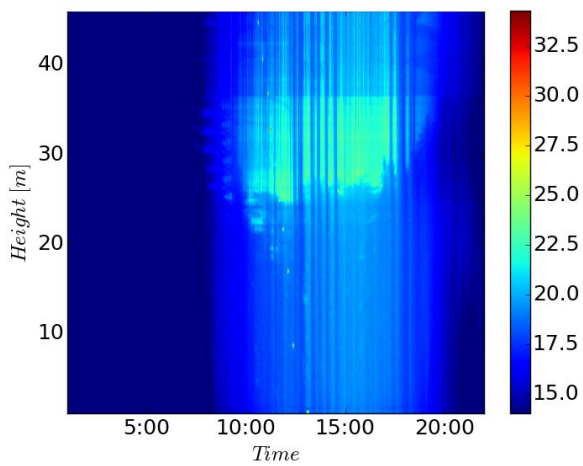


Figure 3 DTS Temperature dry cable on 16-8-16

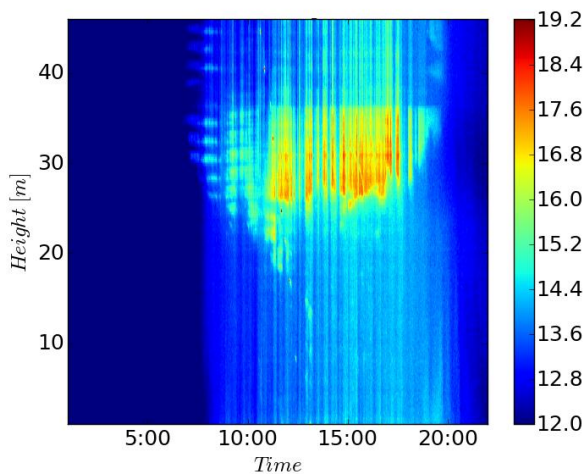


Figure 4 DTS Temperature wet cable on 16-8-16

3.2 Validation DTS temperature

The temperature found with the humidity sensor at height of 4, 16, 24, 32, 38 and 46 m are compared to the DTS temperature of the dry and wet cable at corresponding height. In this chapter the linear regression plots at height 4, 24 and 46 m are presented where 4 m height represents under the canopy, 24 m height in the canopy and 46 m height above the canopy.

3.2.1 Validation dry temperature

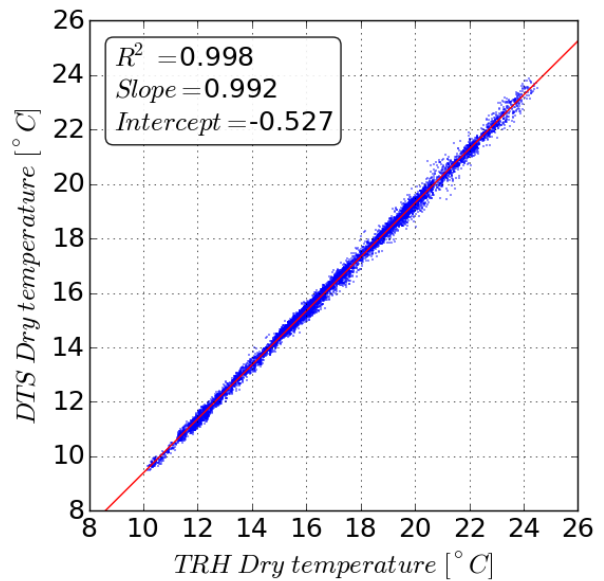


Figure 5 Linear regression of the dry temperature at 4 meters

In figure 5 the linear regression of the dry temperature, measured with the DTS and measured with the relative humidity sensor, at a height of 4 meters is shown. The temperatures match up without large errors.

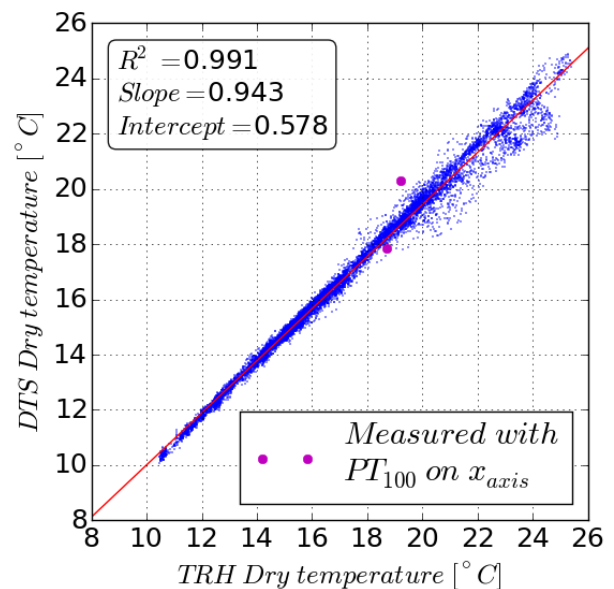


Figure 6 Linear regression of the dry temperature at 24 meters

In figure 6 the linear regression of the dry temperatures at a height of 24 meters is shown. The magenta coloured dots are the manually measured temperatures with the PT100 as explained before in paragraph 2.3.1. The PT100 temperature can be found on the x-axis and is compared with the DTS temperature. The temperatures match up without large errors. A small offset is found which can be due to sensor drift of the temperature probe in the humidity sensor.

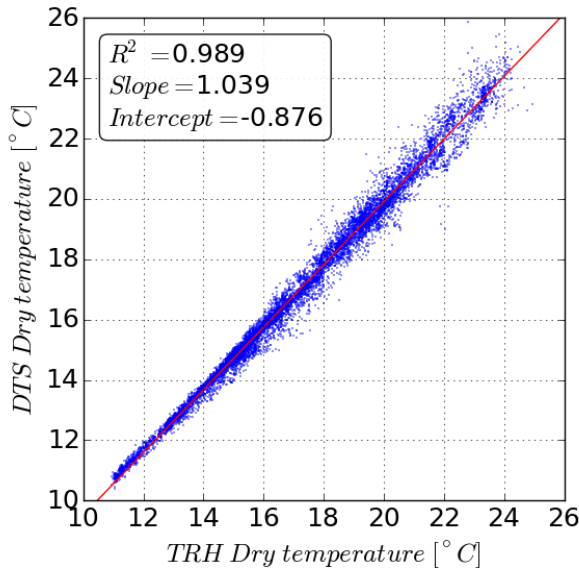


Figure 7 Linear regression of the dry temperature at 46 meters

In figure 7 the linear regression of the dry temperature at a height of 46 meters is shown. The temperatures match up without large errors. Besides the offset and noise in figure 5, 6 and 7 the temperature is nearly one on one with the humidity sensor temperature. In appendix II the linear regression plots of the temperature, measured with the DTS and measured with the relative humidity sensor, at additional heights, 16, 32 and 38 meter, can be found. The slope, offset and R^2 are presented in table 2.

Height	T_{dry}		
	Slope	Offset	R^2
4 m	0.992	-0.527	0.998
16 m	0.995	-0.162	0.998
24 m	0.943	0.578	0.991
32 m	1.194	-3.400	0.979
38 m	1.062	-1.166	0.988
46 m	1.039	-0.876	0.989

Table 2 Linear regression parameters dry temperature

3.2.2 Validation wet temperature

As explained before in paragraph 2.3.2 the wet bulb temperature is derived from the dry bulb temperature and the relative humidity measured with the humidity sensor. This is done by combining Eq. (2) and (3) with Eq. (8) for the equation for the relative humidity (Maidment, 1993). The wet bulb temperature obtained with the humidity sensor is compared to the DTS temperature of the wet cable.

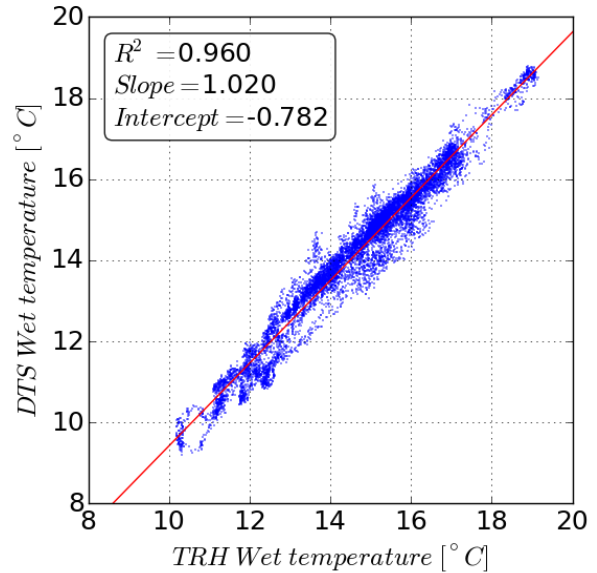


Figure 8 Linear regression of the wet temperature at 4 meters

In figure 8 the linear regression of the wet temperature at a height of 4 meters is shown.

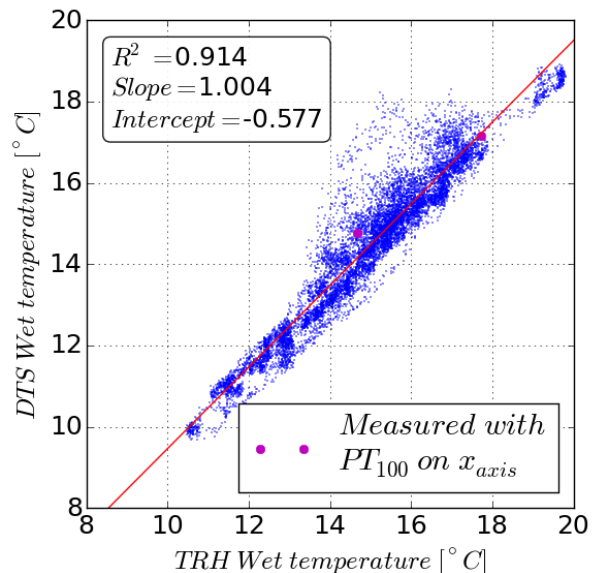


Figure 9 Linear regression of the wet temperature at 24 meters

In figure 9 the linear regression of the wet temperature at a height of 24 meters is shown. The magenta coloured dots are the manually measured temperatures with the PT100 as explained before in paragraph 2.3.1. The PT100 temperature can be

found on the x-axis and is compared with the DTS temperature.

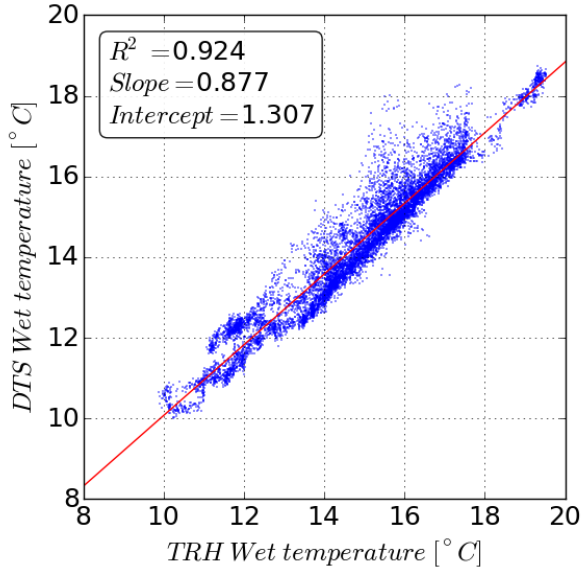


Figure 10 Linear regression of the wet temperature at 46 meters

In figure 10 the linear regression of the wet temperature at a height of 46 meters is shown. More noise is visible than for the dry cable at the same height and also R^2 is lower. In appendix II the linear regression plots of the temperature, measured with the DTS and measured with the relative humidity sensor, at additional heights, 16, 32 and 38 meters, can be found. The slope, offset and R^2 are presented in table 2.

Height	T_{wet}		
	Slope	Offset	R^2
4 m	1.020	-0.782	0.960
16 m	0.981	-0.060	0.988
24 m	1.004	-0.557	0.914
32 m	1.146	-1.976	0.848
38 m	1.045	-0.751	0.953
46 m	0.877	1.307	0.924

Table 3 Linear regression parameters wet temperature

Comparing the temperatures measured with the DTS and the relative humidity sensor demonstrates a near perfect correlation. The correlation changes over the height of the tower, see table 2 and 3. At a height of 32 meters the correlation is, for the dry cables as well as for the wet cable, the least perfect. The height of 32 meters is the only measuring point at which the cable is not shaded by the sunscreen or the trees. Furthermore an additional trend can be found in the correlation, under the canopy the best correlation is found followed by the correlation above the canopy but underneath the sunscreen.

3.4 Energy balance

The energy balance is described in Eq. (9) (Barr at al. 1994).

$$R_N = H + \Delta H + \rho\lambda E + \Delta\rho\lambda E + G_S + G_B + G_P \quad (9)$$

Where ΔH , the vertically integrated flux difference of H between the surface and height z ($W m^{-2}$), is described by Eq. (10).

$$\Delta H = \int_0^z \rho_a c_p \frac{dT_a}{dt} dz \quad (10)$$

And $\Delta\rho\lambda E$ is, the vertically integrated flux difference of $\rho\lambda E$ between the surface and height z ($W m^{-2}$), described by Eq. (11).

$$\Delta\rho\lambda E = \int_0^z \rho_a \lambda \frac{dq}{dt} dz \quad (11)$$

The term G_S , G_B and G_P are the storage terms ($W m^{-2}$) of the energy balance for soil heat, biomass heat and energy used for photosynthesis. Because the storage terms of the energy balance are not measured it is assumed to be one percent of the net radiation.

In Eq. (10) and (11) ρ_a is the density of air ($kg m^{-3}$) and q is the specific humidity ($kg kg^{-1}$) which can be derived with Eq. (12).

$$q = w_s \frac{e_a}{e_s} \quad (12)$$

Where w_s is the mass mixing ratio of water vapor to dry air at equilibrium, it can be calculated with Eq. (13).

$$w_s = \frac{e_s R_d}{R_v (p_{air} - e_s)} \quad (13)$$

In Eq. (13) R_d is the specific gas constant for dry air ($J kg^{-1} K^{-1}$) and R_v is the specific gas constant for water vapor ($J kg^{-1} K^{-1}$).

In figure 11 the sum of the latent and sensible heat flux measured with the EC system (blue line) is compared to the measured energy balance terms (red line) as shown in Eq. (14). Figure 11 is of the first period and in between 36.5 and 38.5 meter. In appendix III the comparisons of the measured energy balance terms of period two and in between different heights is shown. Eq. (14) is obtained from Eq. (9).

$$R_N - \Delta H - \Delta\rho\lambda E - G = H + \rho\lambda E \quad (14)$$

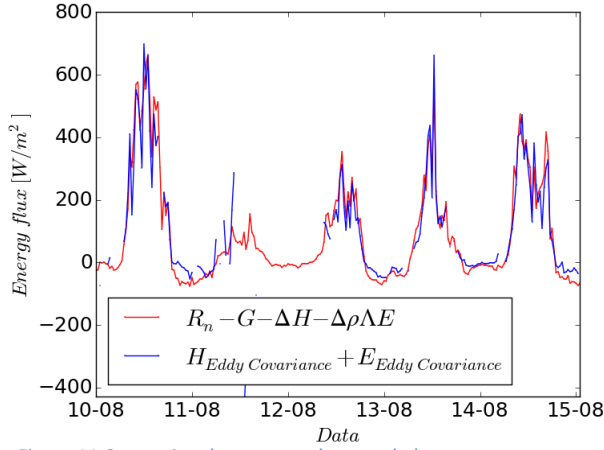


Figure 11 Comparing the measured energy balance terms

The blue and red line look similar which means that, when the assumption for G is realistic, there is no large energy balance gap. Comparing the difference between the net radiation and the EC measured fluxes was also done nine months earlier in October by B. Schilperoort (2015) at the same study site only during this measurement period the screen was not installed yet. During this research the energy gap was quite large. With an increasing gap if the wind direction was coming from the northeast. In the results from this research there is no relationship between wind direction and energy gap.

Figure 12 presents the latent heat flux measured with the EC system (red line) and the blue line presents the latent heat flux obtained with the Bowen ratio, found with the DTS, combined with measurements for R_n and G as shown in (Eq.6). Figure 12 is of the first period and in between 36.5 and 38.5 meter. In appendix III the comparisons of the latent heat fluxes of period two and in between different heights is shown.

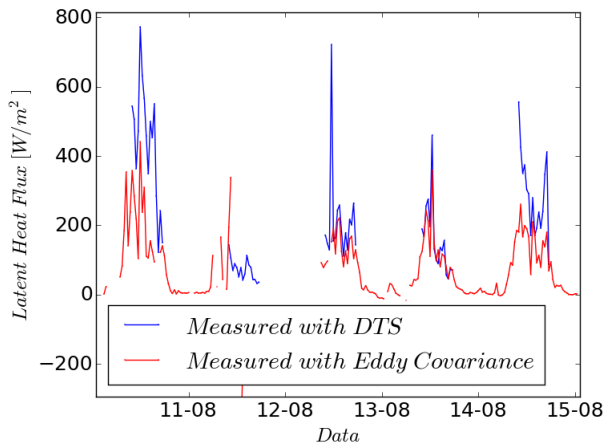


Figure 12 Latent heat flux determined with the BR-DTS method (bleu) and the EC method (red).

The red and blue line in the figure 12 follow the same pattern, during the day the latent heat fluxes become larger and during the night it goes to zero.

The latent heat flux measured with the EC system has smaller peaks. During the largest peak, on the 11th of August, the difference between the fluxes obtained with the two methods is more than 300 W m^{-2} . The fact that the latent heat flux measured with the BR-DTS setup is greater than the latent heat flux measured with the EC setup is similar to the results from B. Schilperoort (2015).

Figure 13 shows the sensible heat flux measured with the EC system (red line) and the blue line presents the sensible heat flux obtained with the Bowen ratio, found with the DTS, combined with measurements for R_n and G . In figure 13 the first period is shown in between 36.5 and 38.5mheight. In appendix III the comparisons of the sensible heat fluxes of period two and in between different heights can be found.

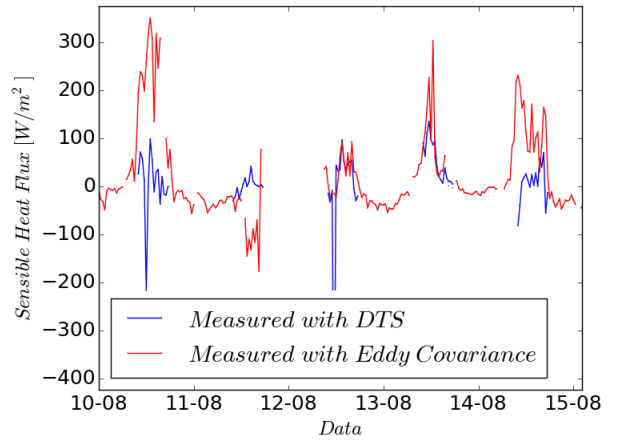


Figure 13 Sensible heat fluxes determined with the BR-DTS method (bleu) and the EC method (red).

The different methods for obtaining the sensible heat flux show less similarity as the different methods for the latent heat flux. In figure 13 the sensible heat flux measured with the EC system has larger peaks but on the other hand the sinks of the sensible heat flux obtained with the DTS are larger. On the 12th of August the difference in sensible heat flux goes up to almost 600 W m^{-2} .

The fact that the sensible heat flux measured with the BR-DTS setup is smaller than the sensible heat flux measured with the EC setup is in contradiction with the results from B. Schilperoort (2015).

4 Conclusion

The aim of this study was at first to verify if the temperature data of the dry and wet cable are correct and second to compare the outcome with the EC data. The temperature of the dry and wet cable measured with the BR-DTS method are really close to the temperatures measured with the relative humidity sensors with a maximum R^2 of 0.998 at 4 and 16 meter height for the dry cable and a maximum R^2 of 0.988 at 16 meter height for the wet cable. The energy gap found is relatively small

which is in contrast with B. Schilperoort (2015) just as the absence of a relationship between the wind direction and the energy gap is in contradiction with B. Schilperoort (2015). The latent heat flux measured with the BR-DTS setup is just as in the results from B. Schilperoort (2015) greater than the latent heat flux measured with the EC setup on the other hand the sensible heat flux measured with the BR-DTS setup is smaller than the sensible heat flux measured with the EC setup which is in contradiction with the results from B. Schilperoort (2015).

5 Recommendations

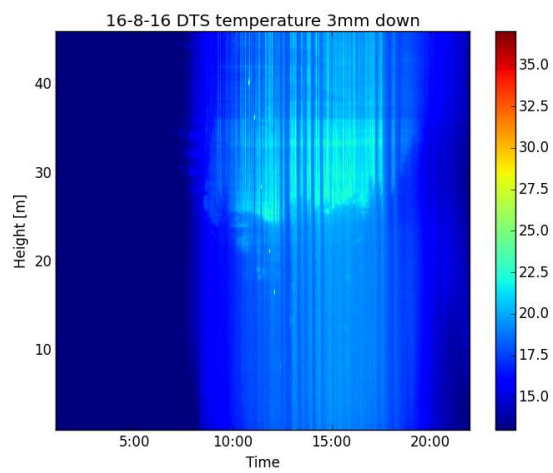
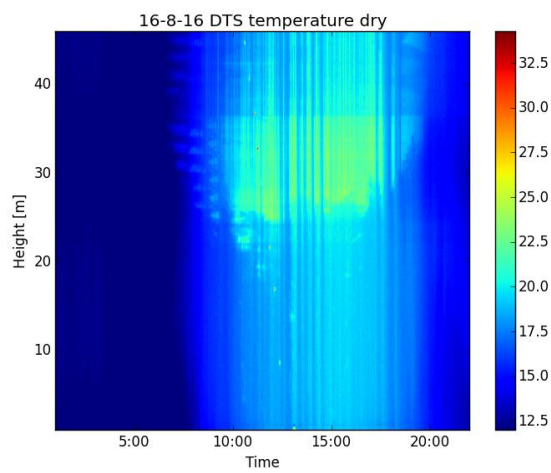
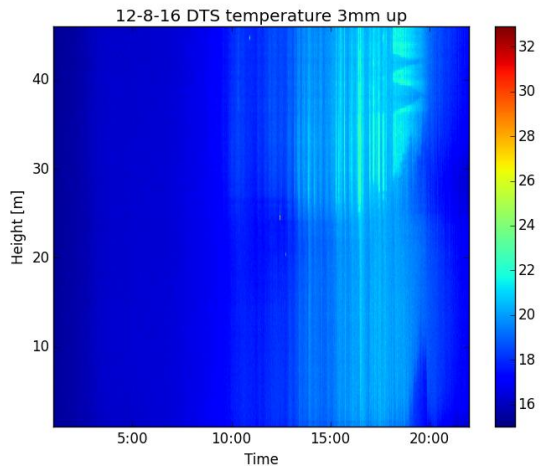
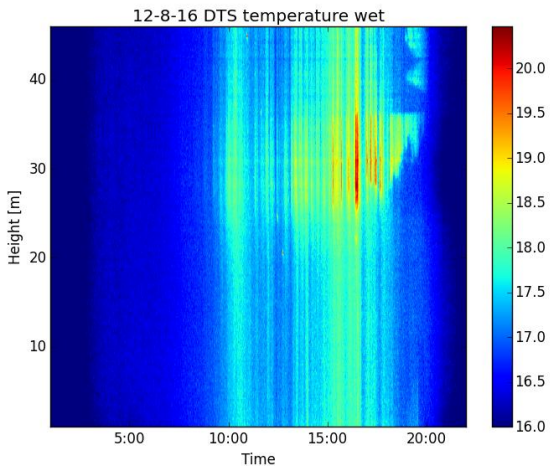
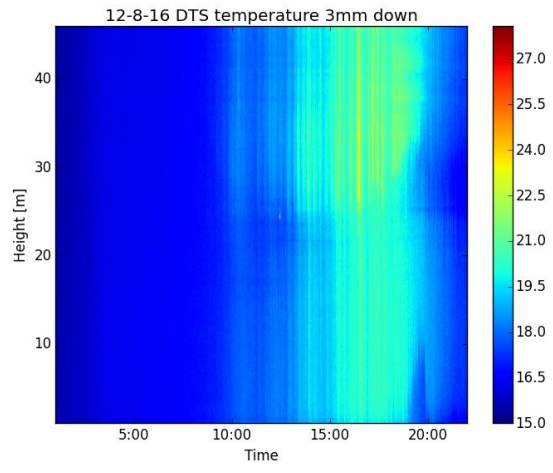
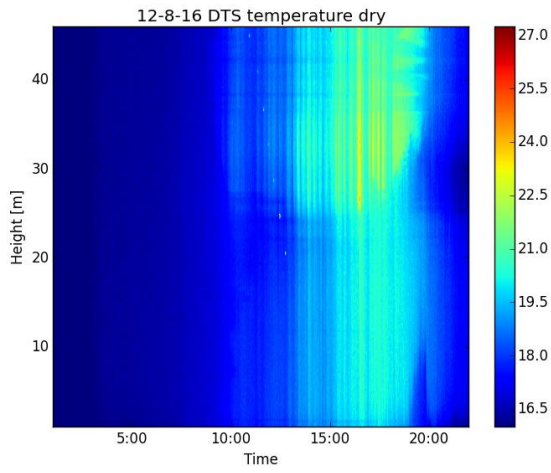
The results clearly show that the sunscreen can be improved and that this will lead to a better correlation of the DTS temperature with the temperature measured with the relative humidity sensor. Therefore one of the most important recommendations is to change the sunscreen in a way that the cable is also shaded in the morning, when the sun comes up from the east and in a way that the cable is shaded over the whole length. For this the sunscreen needs to start from around 27 meter height and cover instead of a 180° angle a larger angle. During the 23rd of August the air temperature was that high that the water supply to the wet cable was not enough to fully wetten the cable all the way from the top to the bottom. For further studies a higher water supply during warm days is recommended. Another aspect which is important is the way the EC data is analysed. For this study the Eddy Pro Software is used. In future research it is advisable to further study what exactly happens with the data in the Eddy Pro Software.

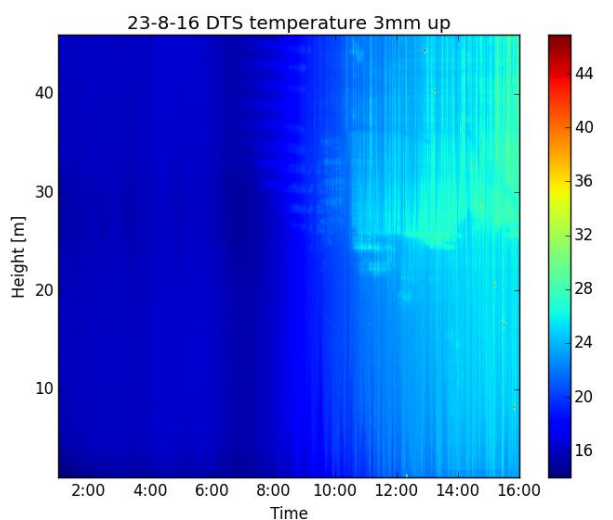
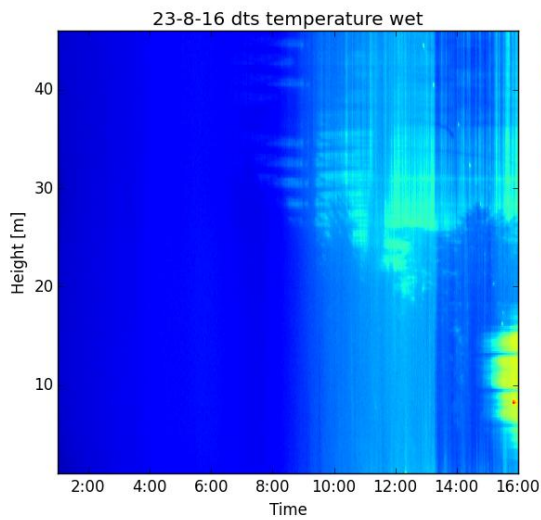
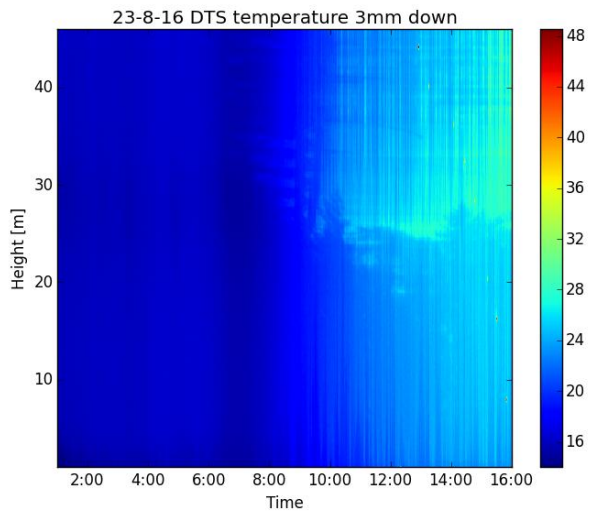
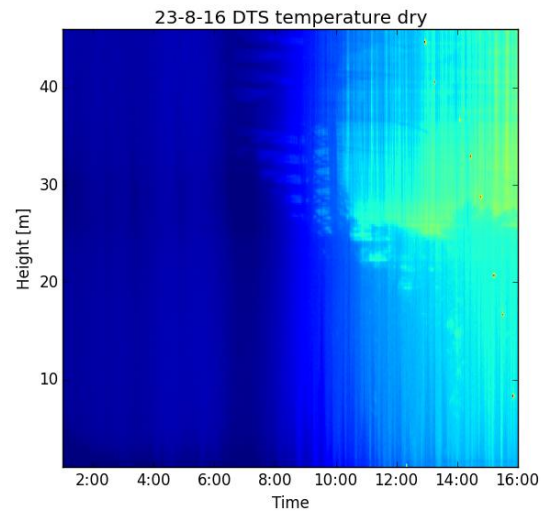
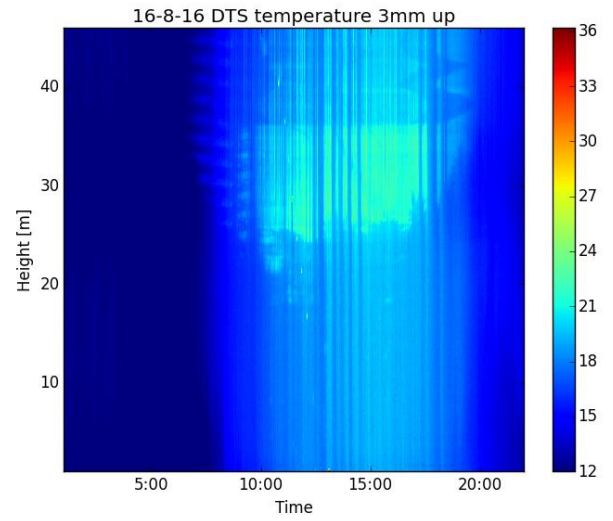
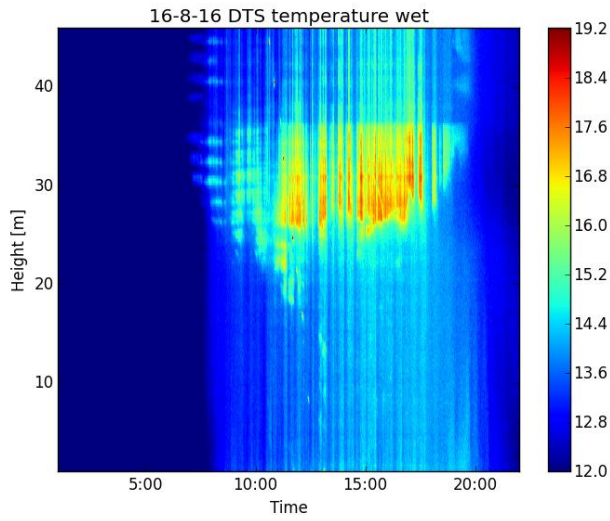
References

- Allen, R. G., Pereira, L. S., Raes, D., and Smith, M.: Crop evaporation – Guidelines for computing crop water requirements, vol. 56, FAO – Food and Agriculture Organization of the United Nations, Rome 1998.
- Angus, D. E. and Watts, P. J.: Evapotranspiration – How good is the Bowen ratio method?, *Agr. Water Manage.*, 8, 133–150, 1984.
- Aston, A. R.: The effect of vertical separation of psychrometers on the determination of Bowen ratios over a young eucalypt forest, *Agr. Forest Meteorol.*, 35, 299–307, 1985.
- Bohren, C. F., and Albrecht, B. A.: *Atmospheric Thermodynamics*. New York, NY: Oxford University Press, 1998.
- Bowen, I. S.: The ratio of heat losses by conduction and by evaporation from any water surface, *Phys. Rev.*, 27, 779–787, 1926.
- Burba, G.: *Eddy Covariance Method for Scientific, Industrial, Agricultural and Regulatory Applications: a Field Book on Measuring Ecosystem Gas Exchange and Areal Emission Rates*, LI-COR Biosciences, Lincoln, USA, 331 pp, 2013.
- Euser, T., Luxemburg, W. M. J., Everson, C. S., Mengistu, M. G., Clulow, A. D., and Bastiaanssen, W. G. M.: A new method to measure Bowen ratios using high-resolution vertical dry and wet bulb temperature profiles, *Hydrol. Earth Syst. Sci.*, 18, 2021–2032, doi:10.5194/hess-18-2021-2014, 2014.
- Fritschen, L. J.: Accuracy of evapotranspiration determinations by the Bowen ratio method, *IAHS Bull.*, 10, 38–48, 1965.
- Foken, T.: The energy balance closure problem: an overview, *Ecol. Soc. Am.*, 18, 1351–1367, 2008.
- Fritschen, L. J. and Simpson, J. R.: Surface energy balance and radiation systems: general description and improvements, *J. Appl. Meteorol.*, 28, 680–689, 1989.
- Gavilán, P. and Berengena, J.: Accuracy of the Bowen ratio-energy balance method for measuring latent heat flux in a semiarid advective environment, *Irrig. Sci.*, 25, 127–140, 2007.
- KNMI: *Bosaltas van het klimaat*, Noordhoff, Groningen, 2011
- Maidment, D.R.: *Handbook of Hydrology*, McGraw-Hill Education, New York City, 1993.
- Perez, P. J., Castellvi, F., Ibañez, M., and Rosell, J. I.: Assessment of reliability of Bowen ratio method for partitioning fluxes, *Agr. Forest Meteorol.*, 97, 141–150, 1999
- Schilperoort, B.: Verifying the distributed temperature sensing Bowen ratio method for measuring evaporation, Technical University of Delft, 2015
- Selker, J. S., Thévenaz, L., Huwald, H., Mallet, A., Luxemburg, W., van de Giesen, N., Stejskal, M., Zeman, J., Westhoff, M., and Parlange, M.B.: Distributed fiber-optic temperature sensing for hydrologic systems, *Water Resour. Res.*, 42, W12202, doi:10.1029/2006WR005326, 2006
- Silixa: 2015, Ultima DTS data sheet, retrieved from: <http://www.silixa.com/wp-content/uploads/ULTIMA-DTS-DATASHEET.pdf>

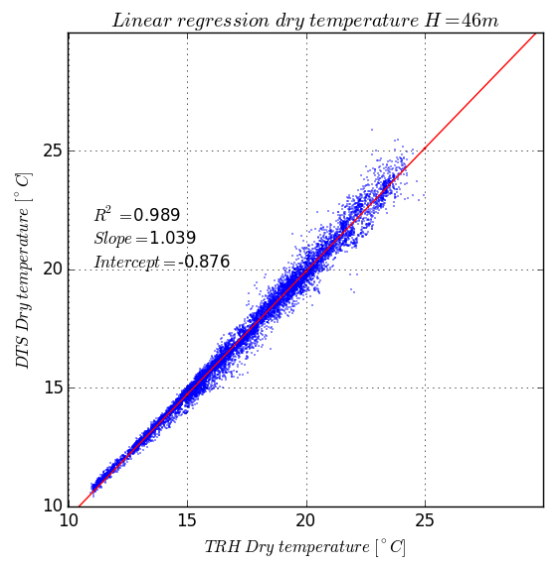
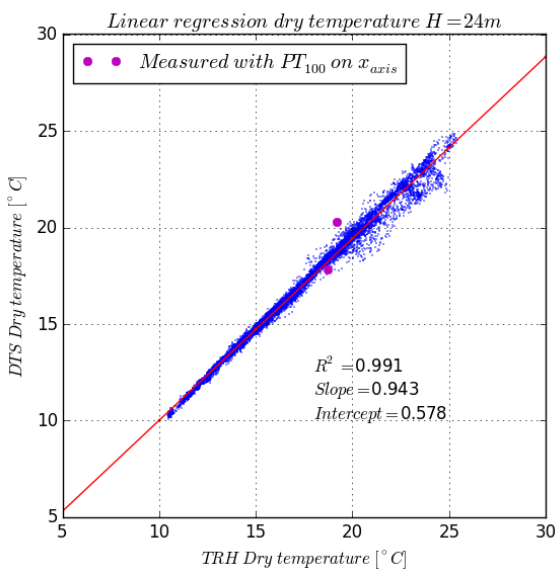
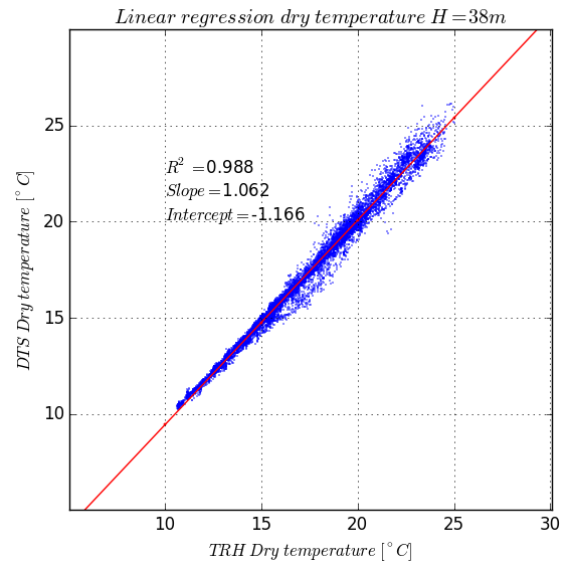
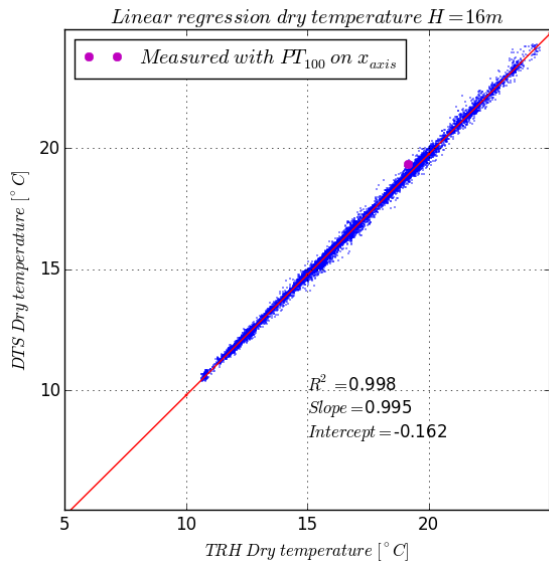
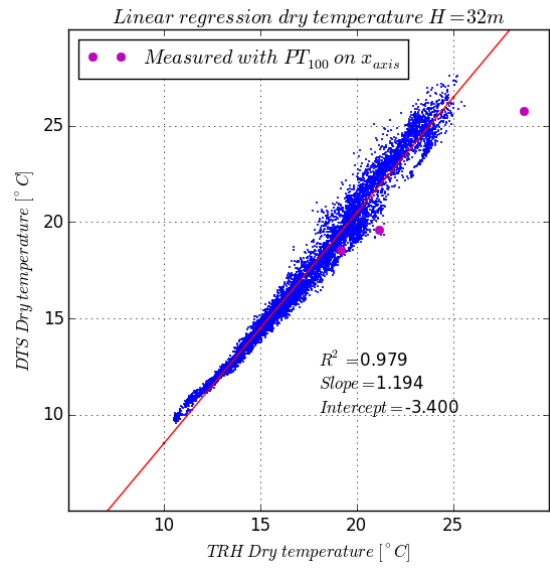
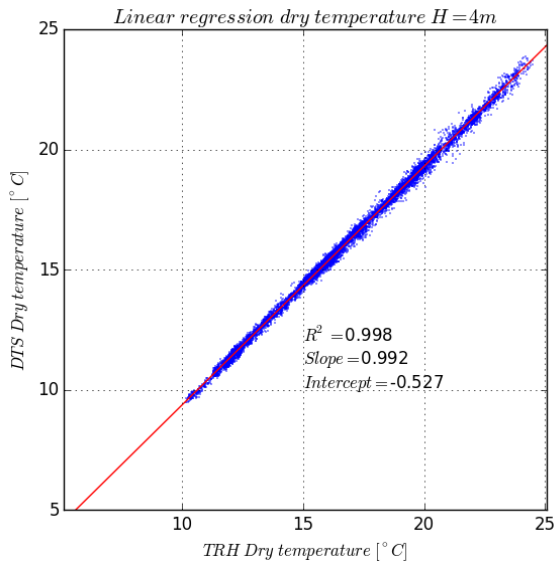
Spittlehouse, D. L. and Black, T. A.: Evaluation of the Bowen ratio/energy balance method for determining forest evapotranspiration, *Atmos. Ocean*, 18, 98–116, 1980.

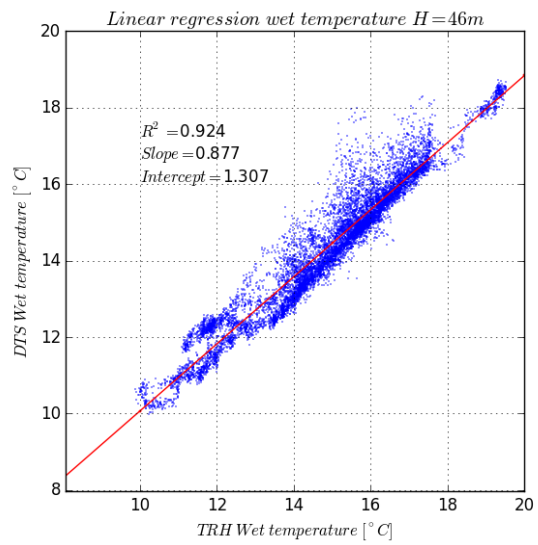
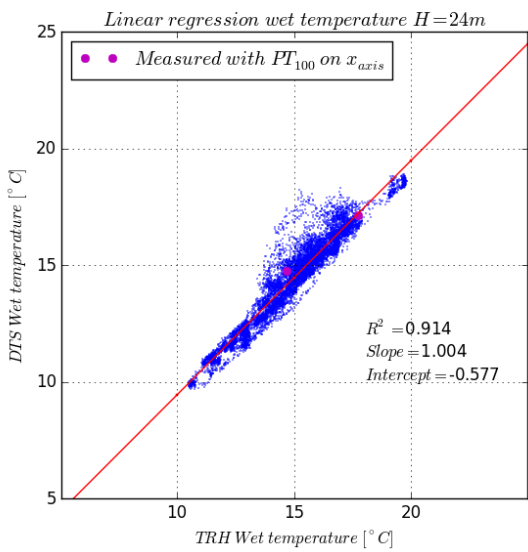
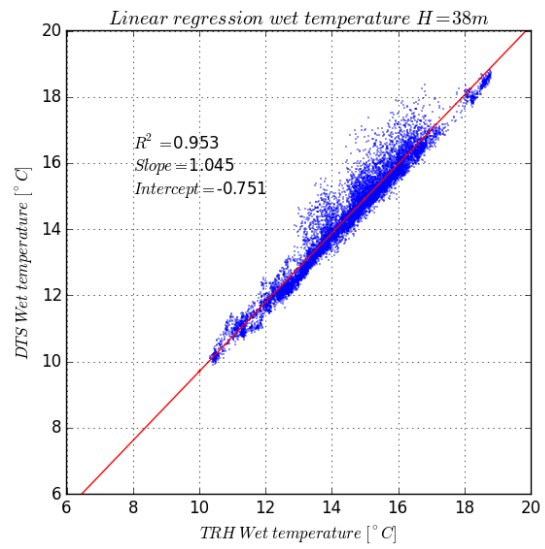
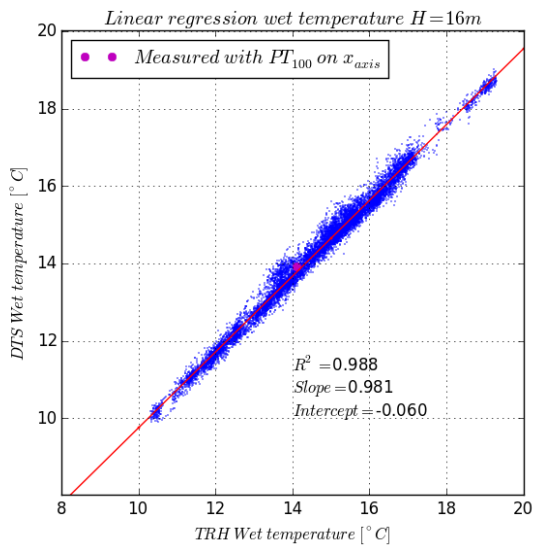
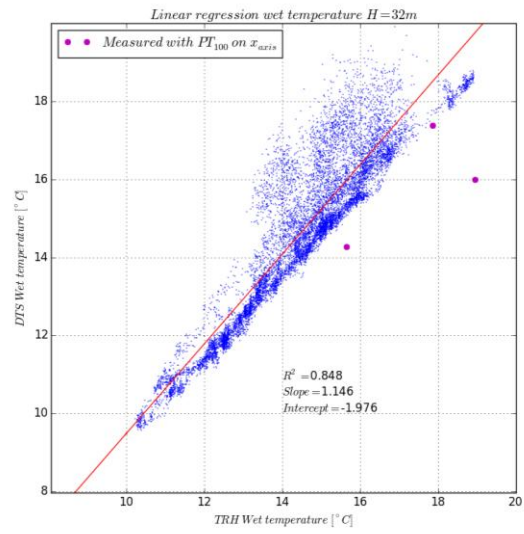
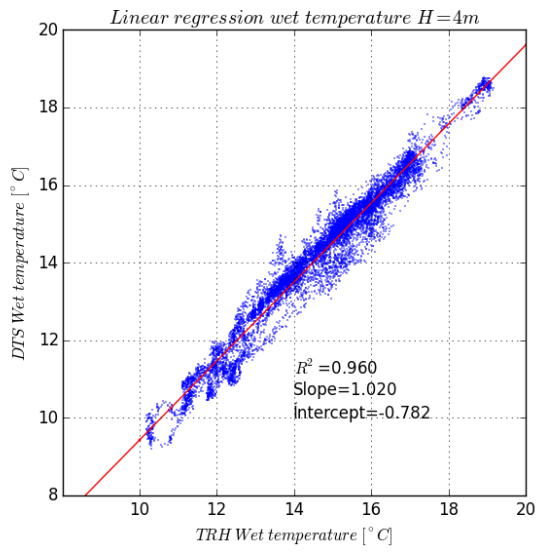
Appendix I



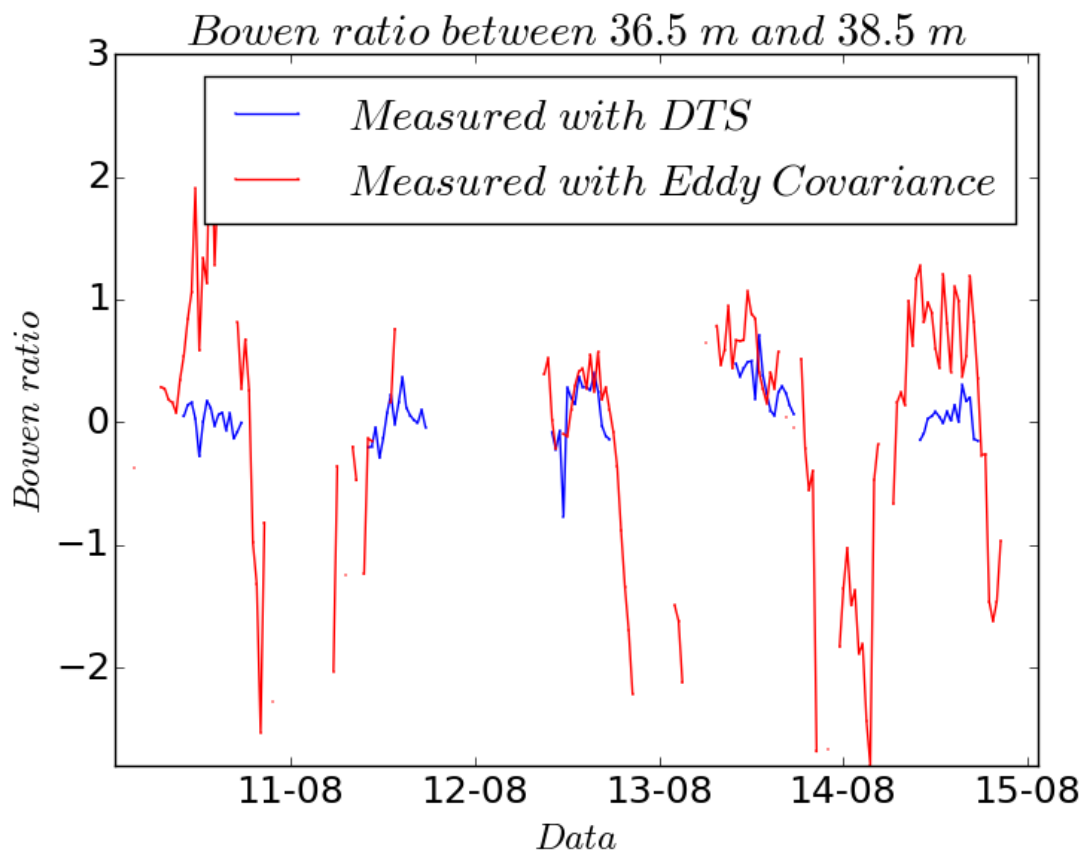
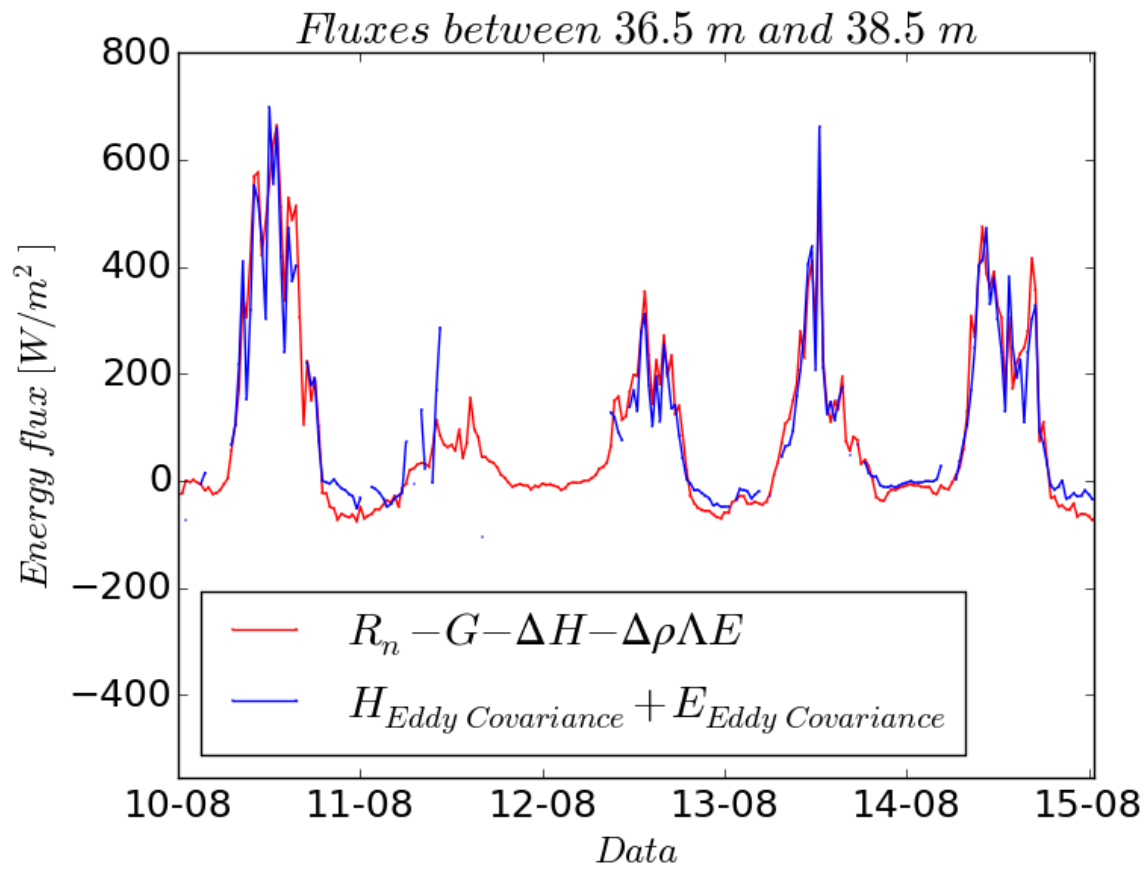


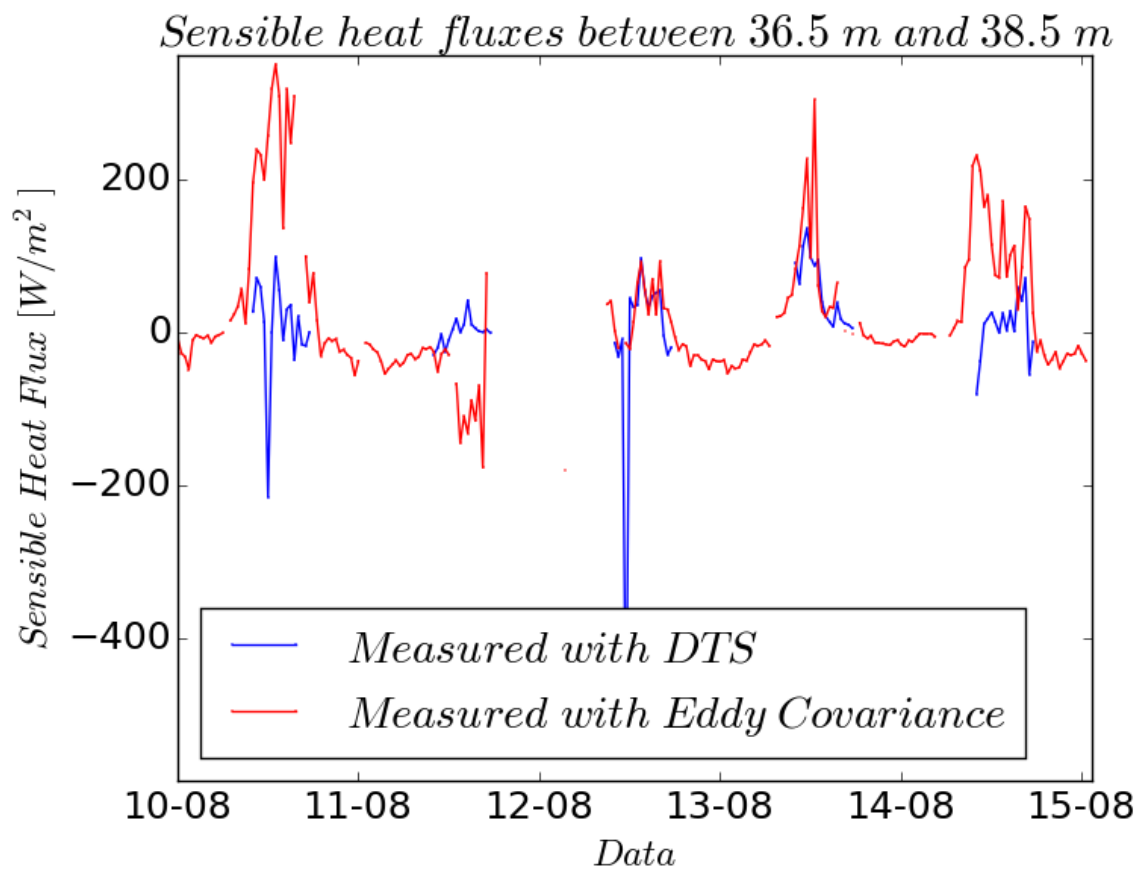
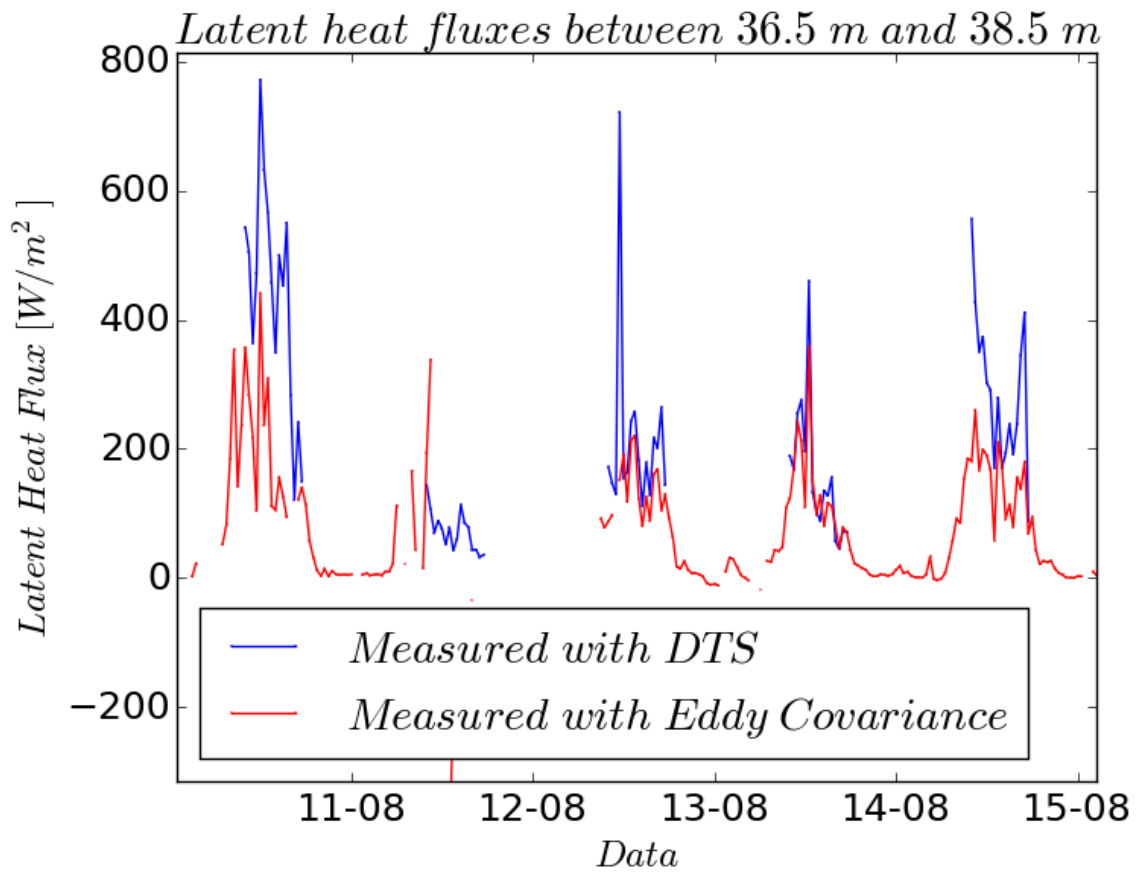
Appendix II

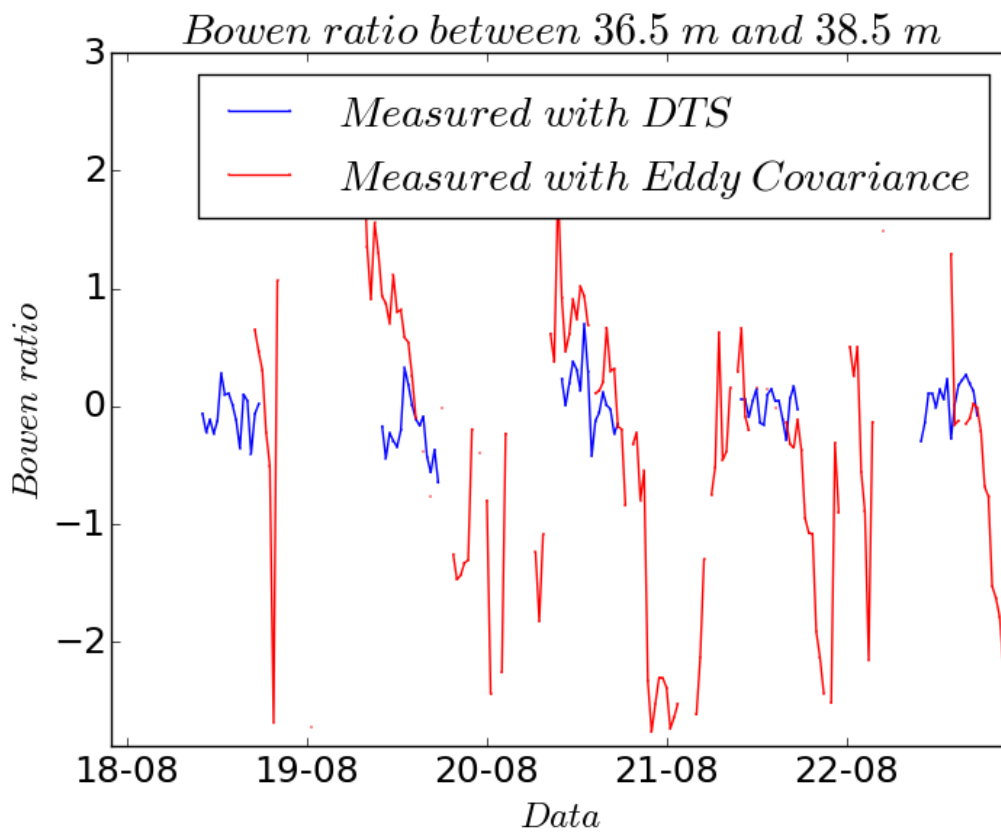
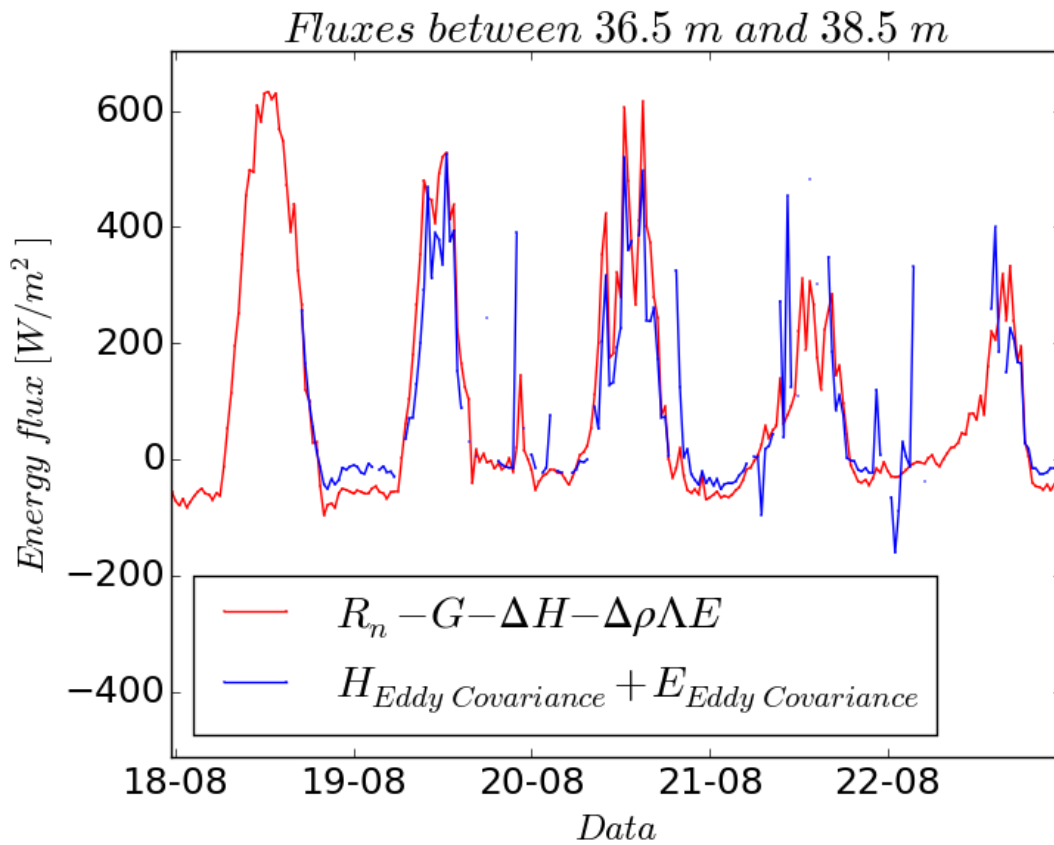




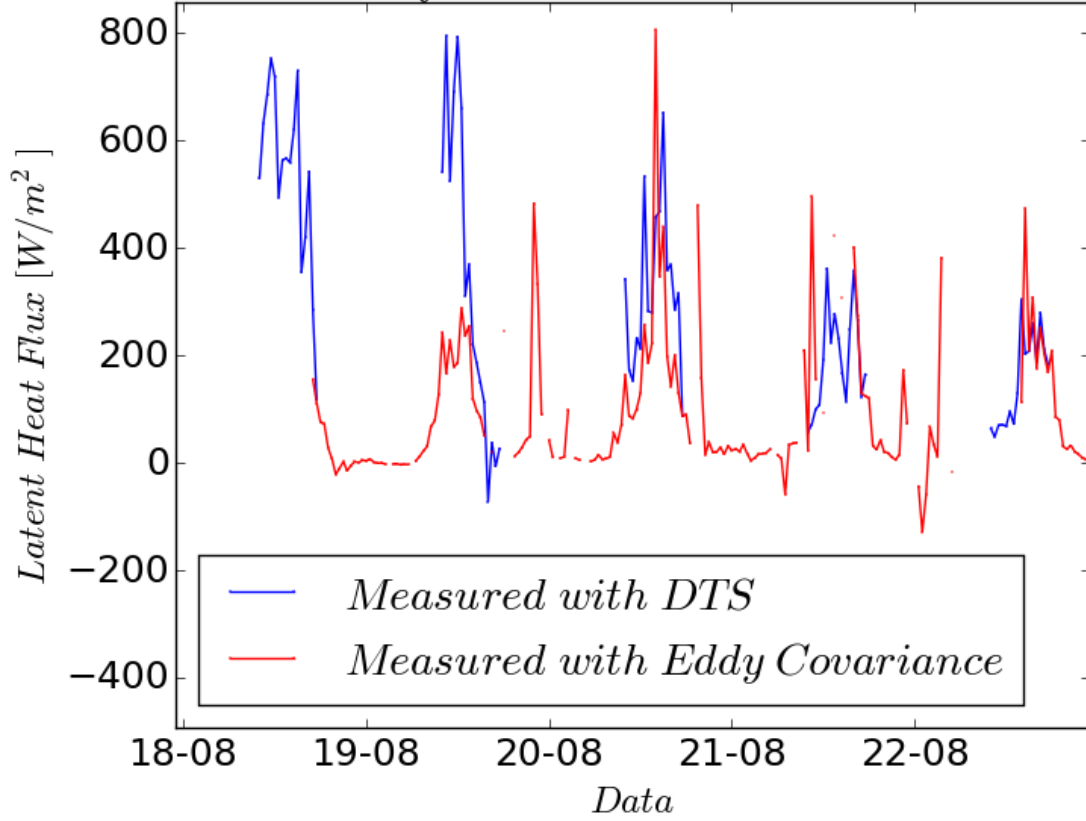
Appendix III



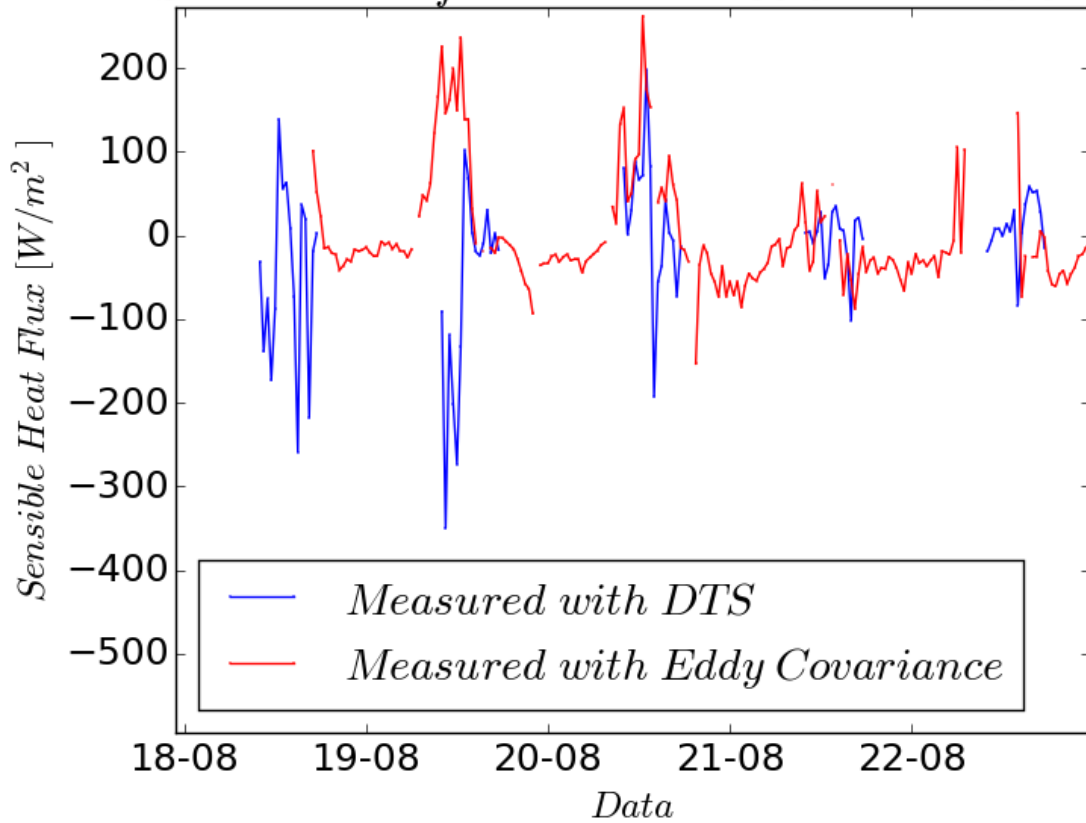


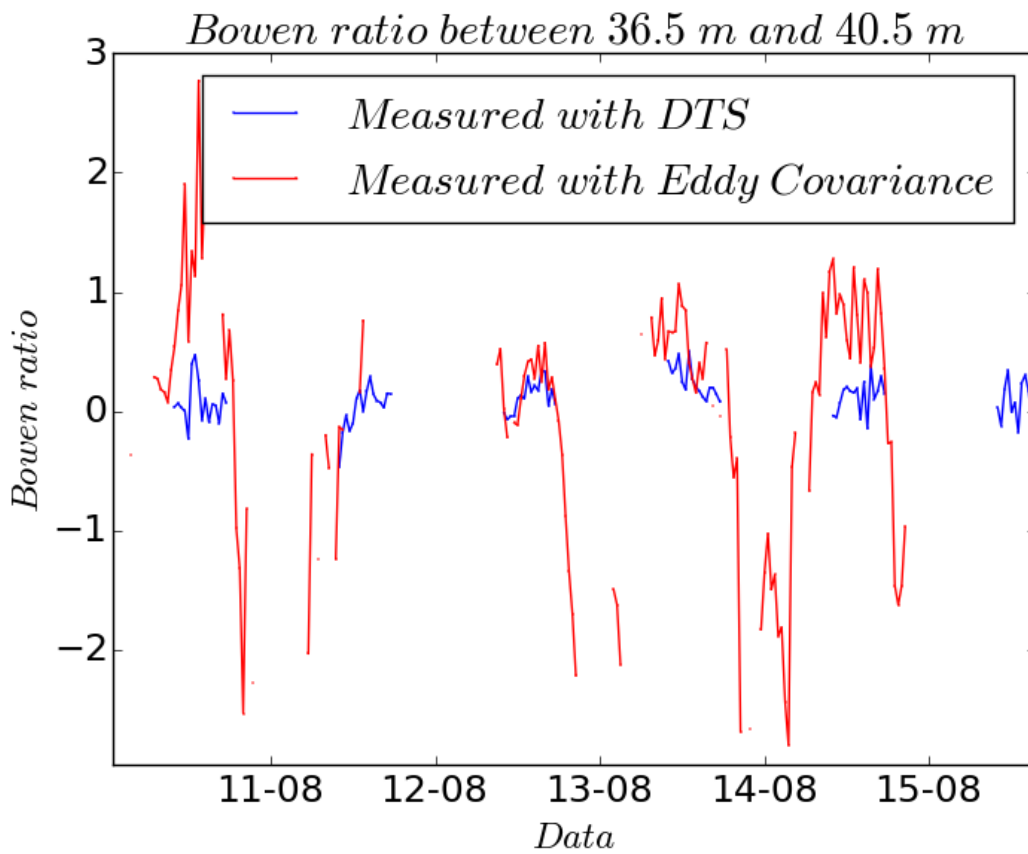
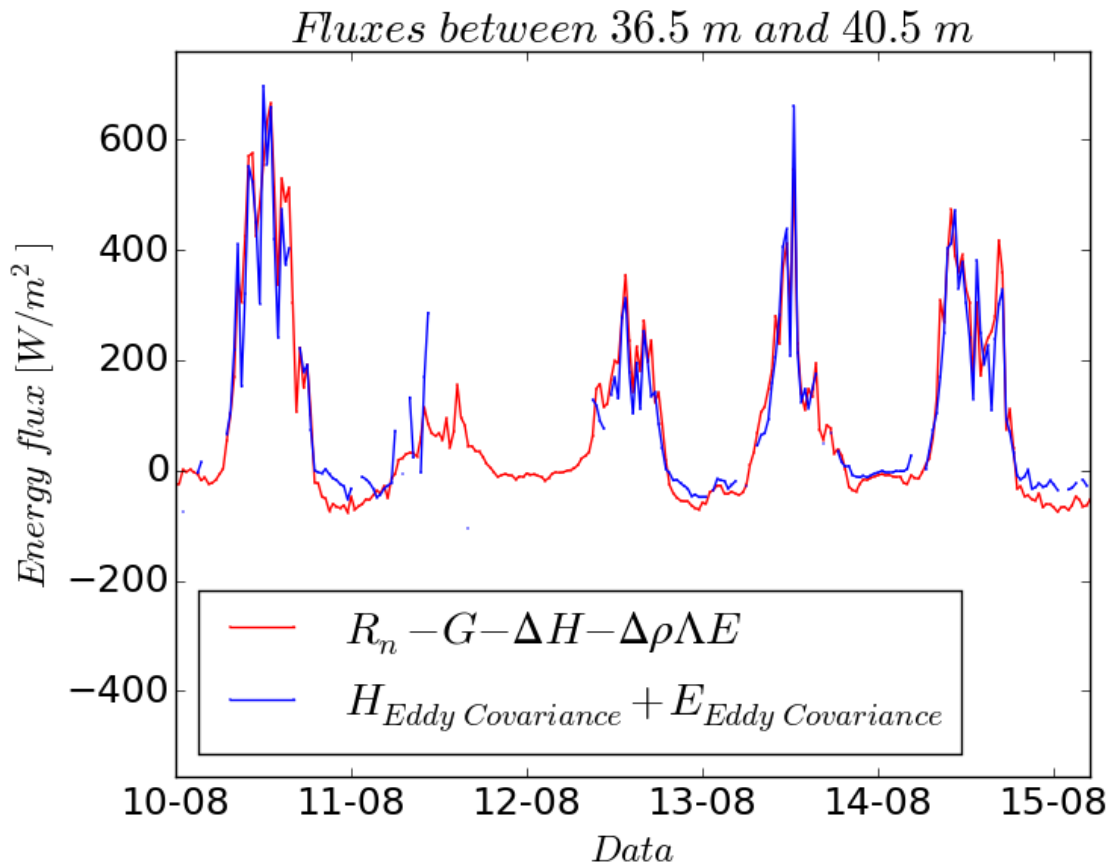


Latent heat fluxes between 36.5 m and 38.5 m

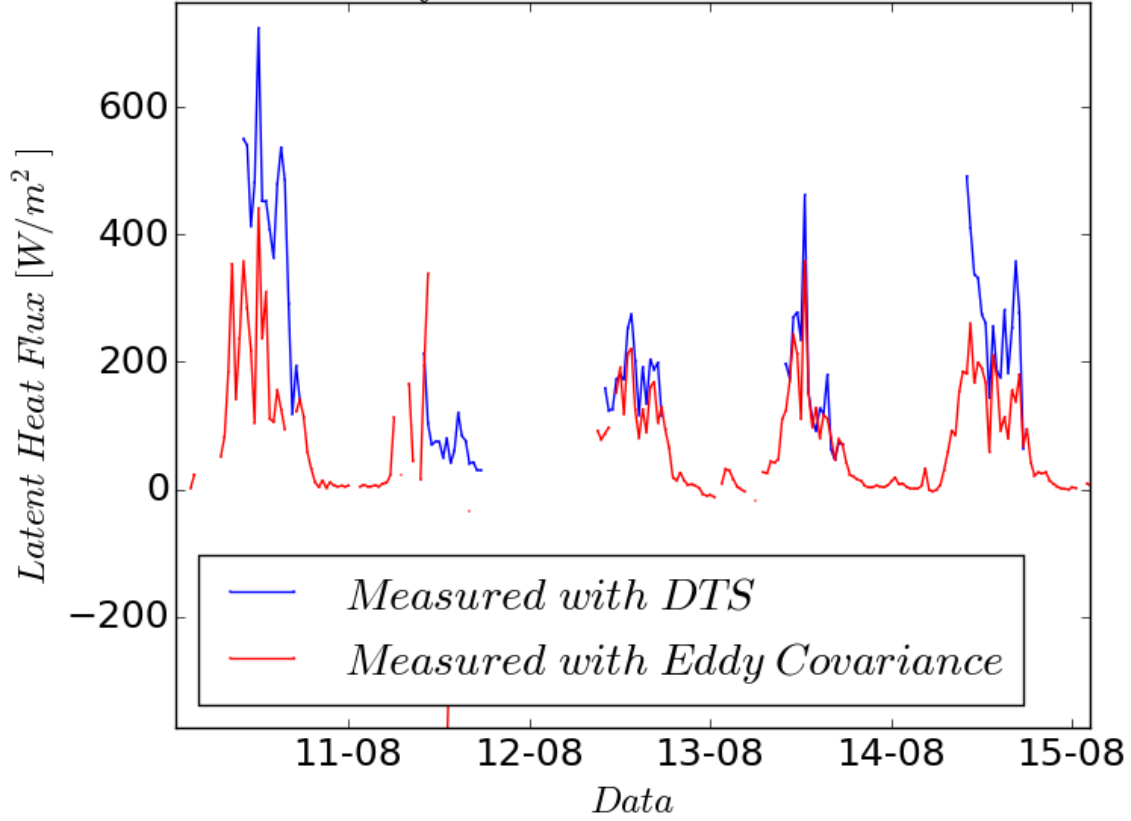


Sensible heat fluxes between 36.5 m and 38.5 m

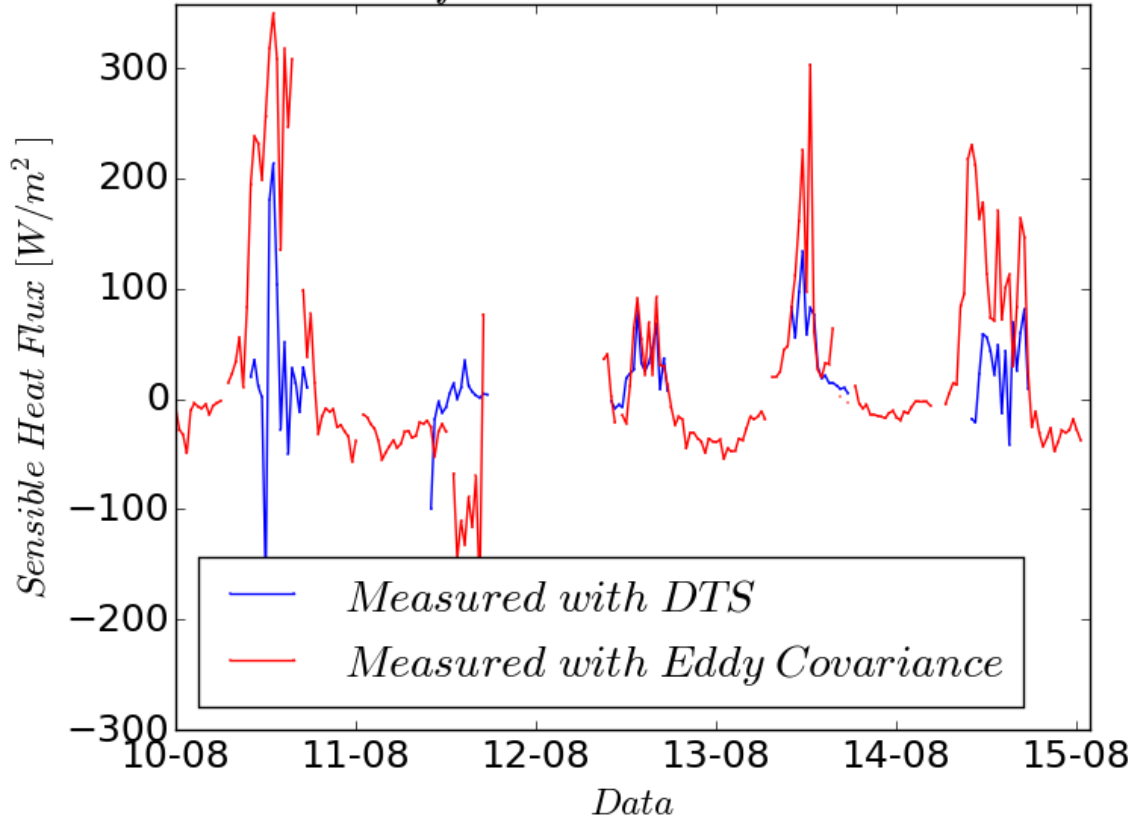


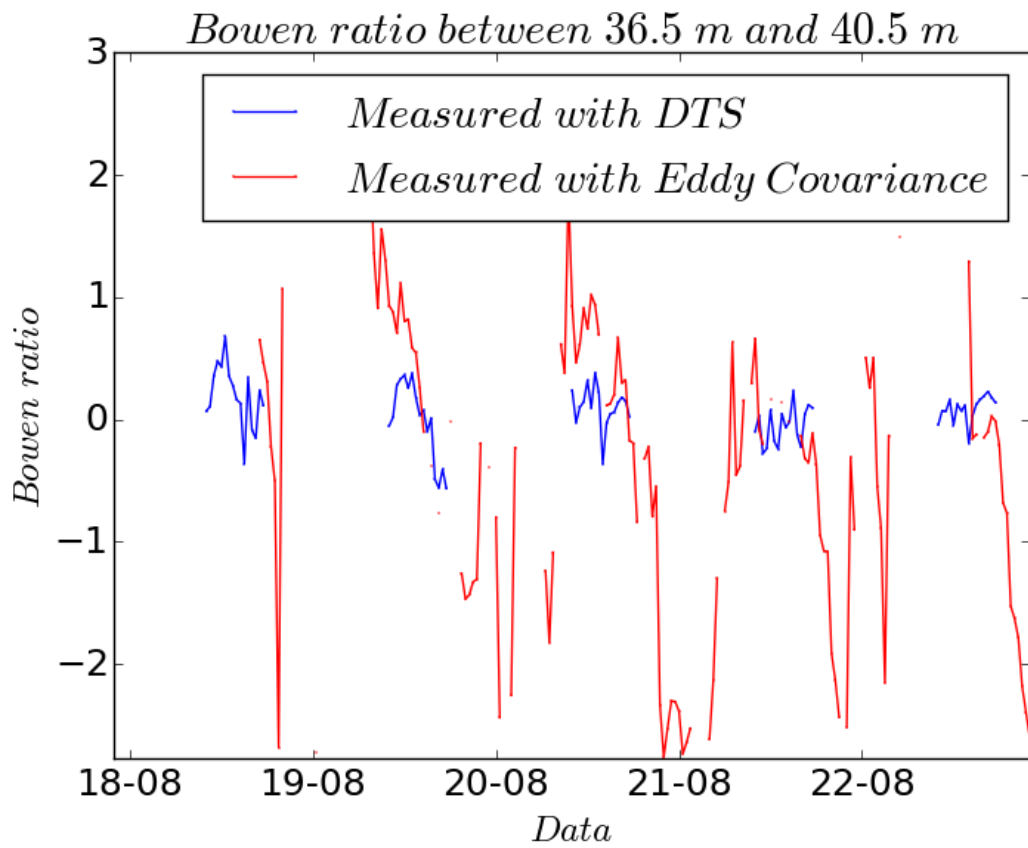
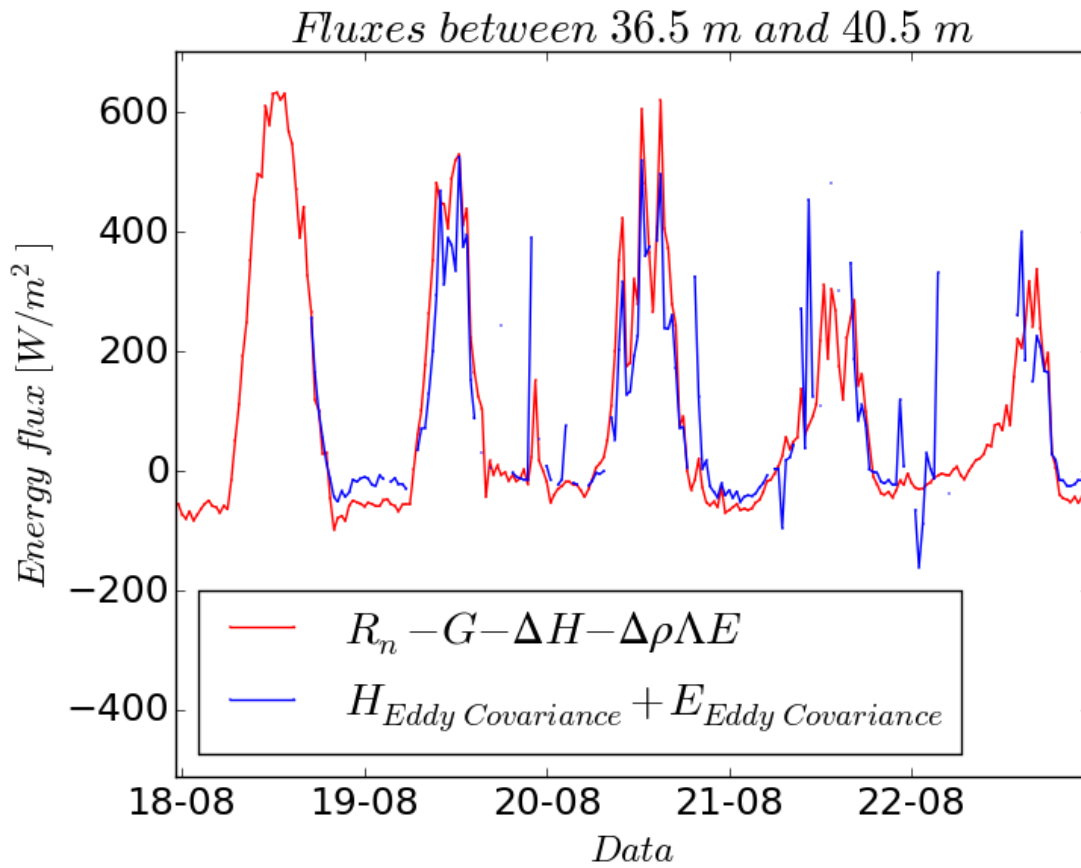


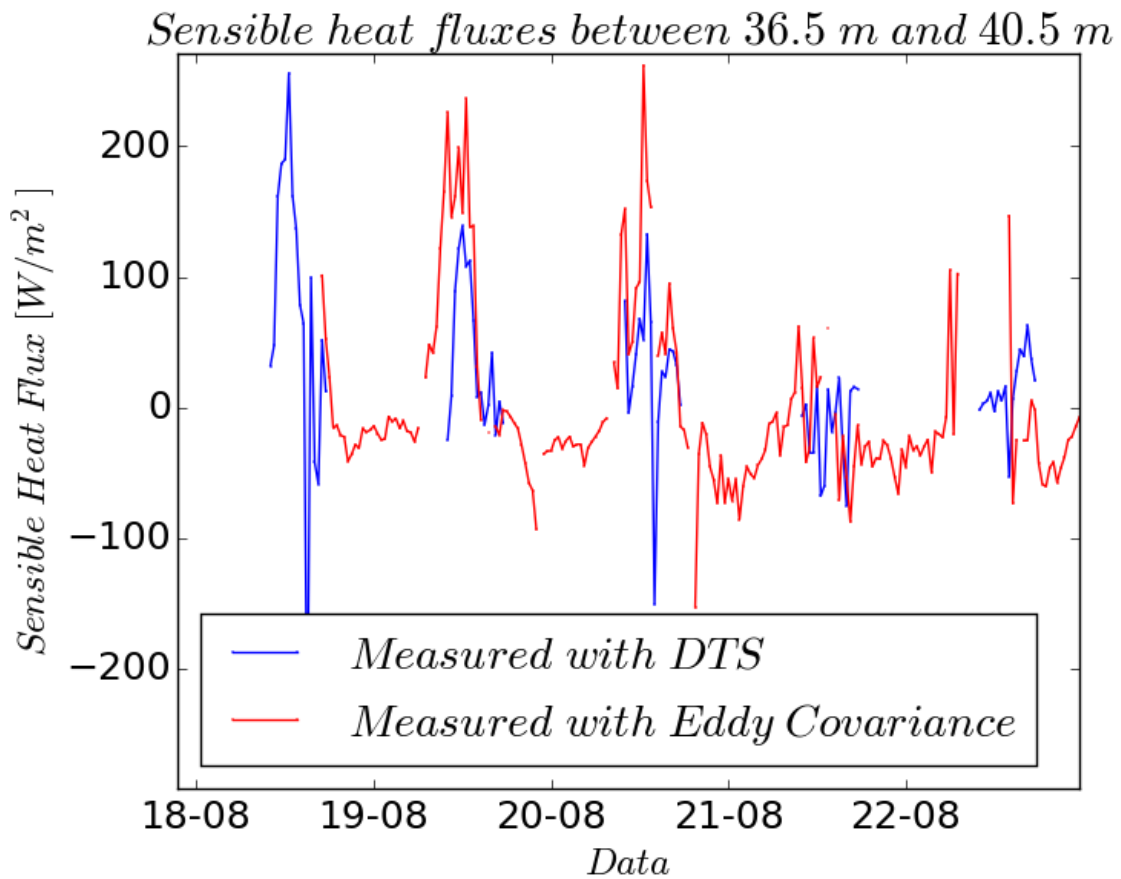
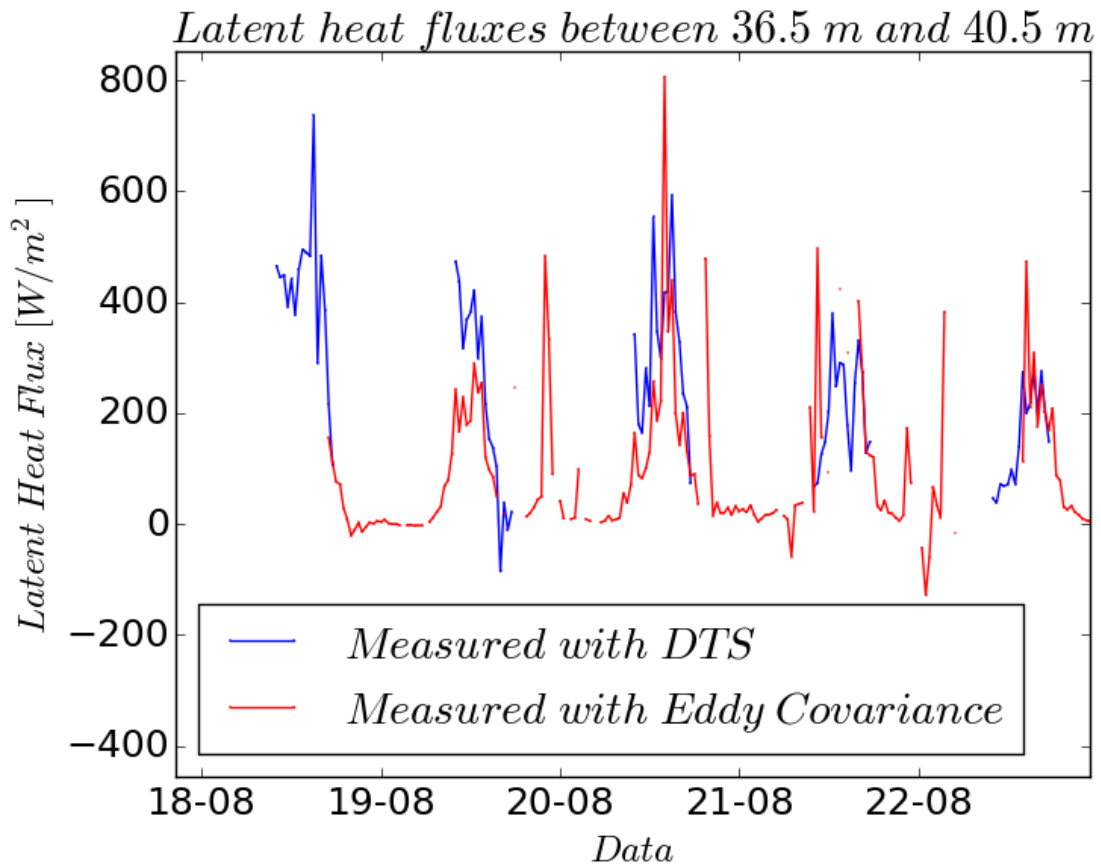
Latent heat fluxes between 36.5 m and 40.5 m

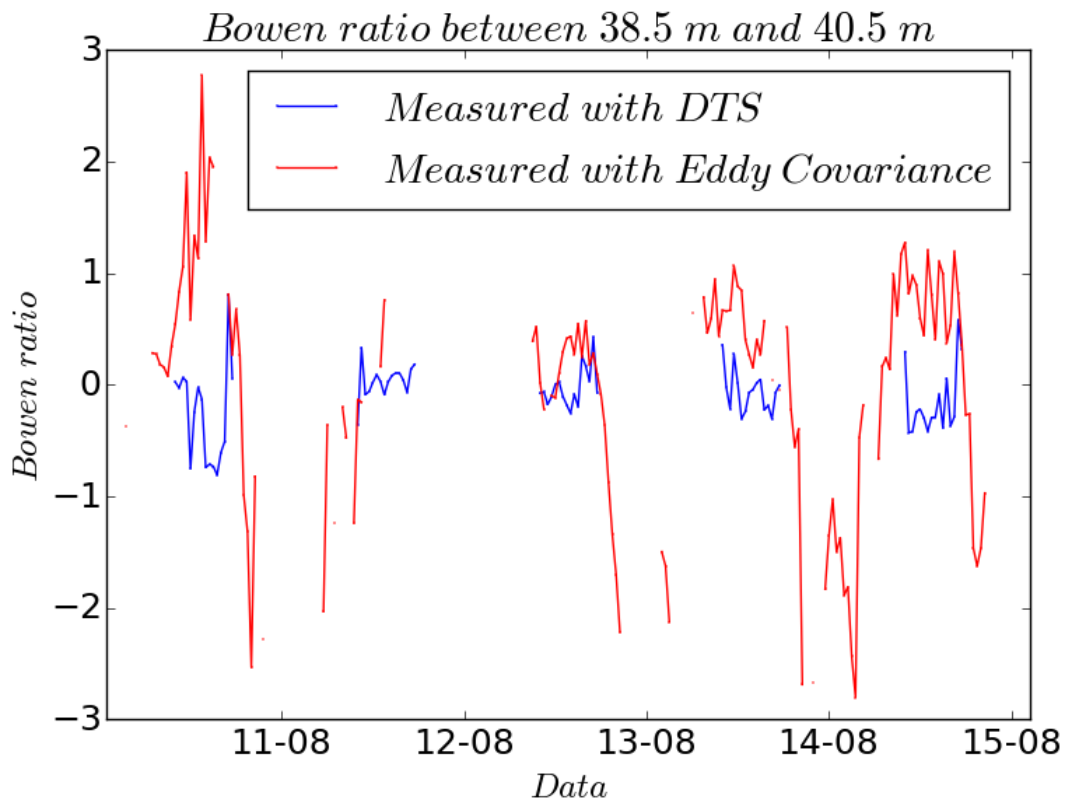
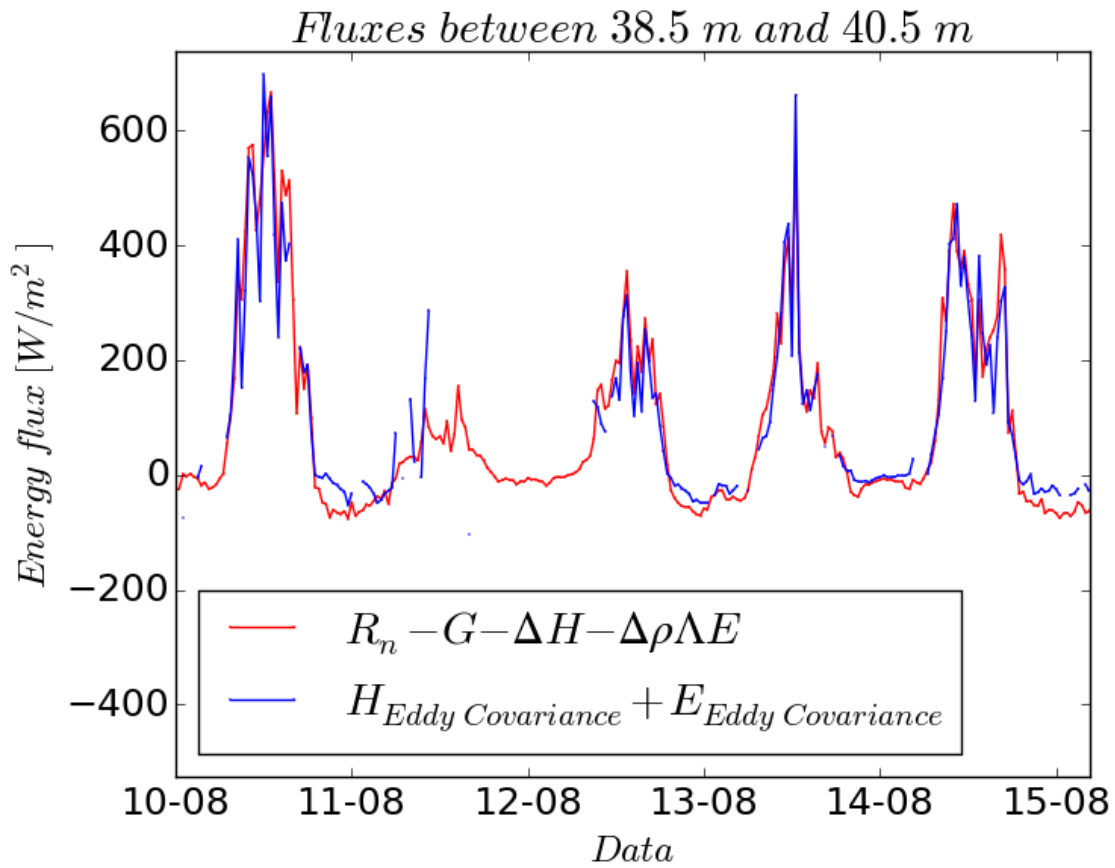


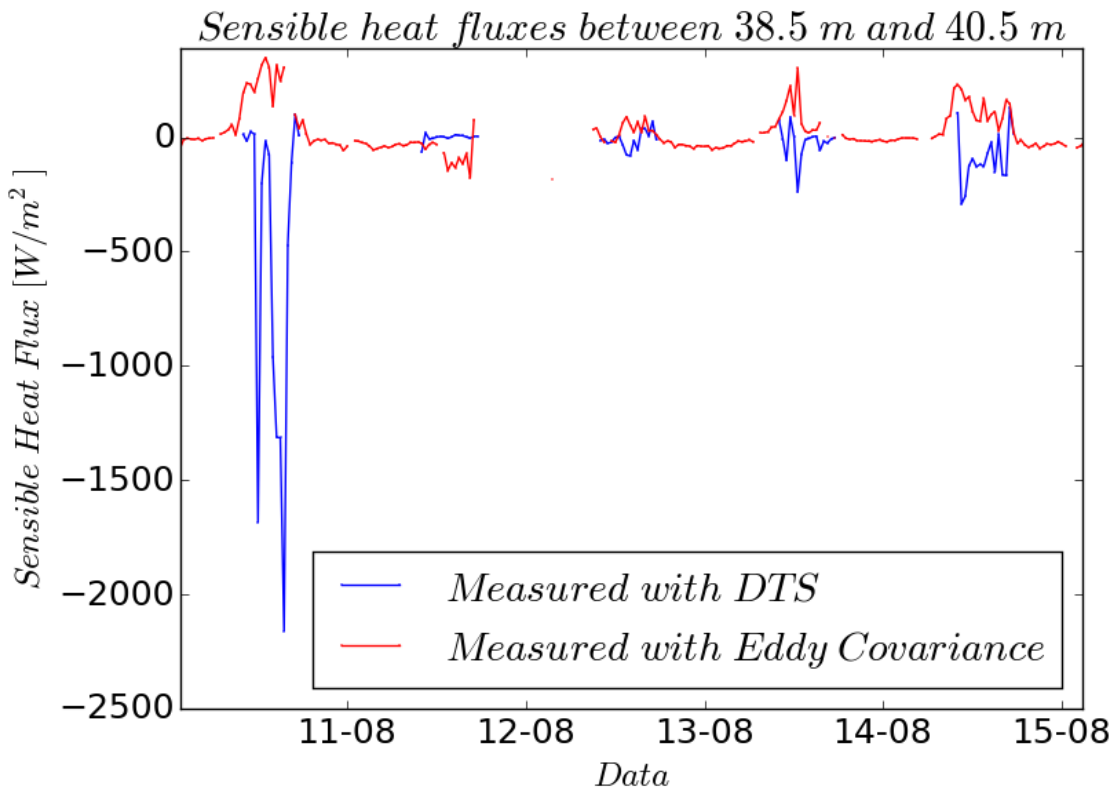
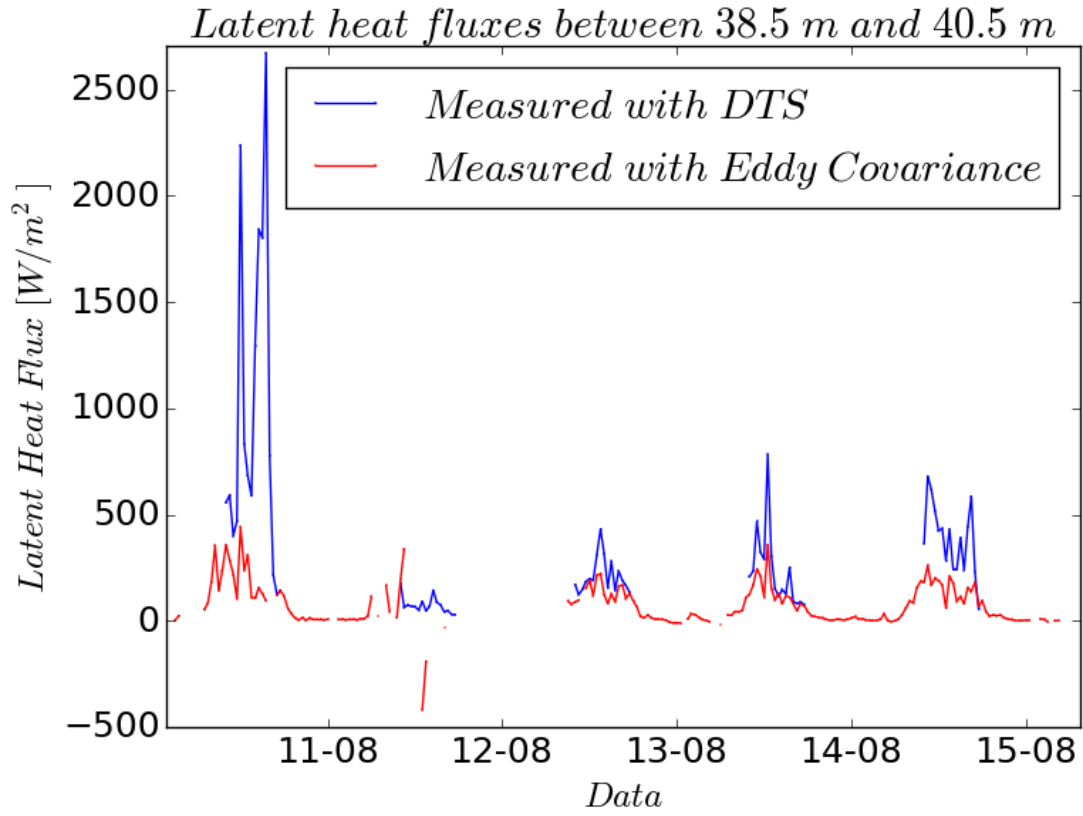
Sensible heat fluxes between 36.5 m and 40.5 m

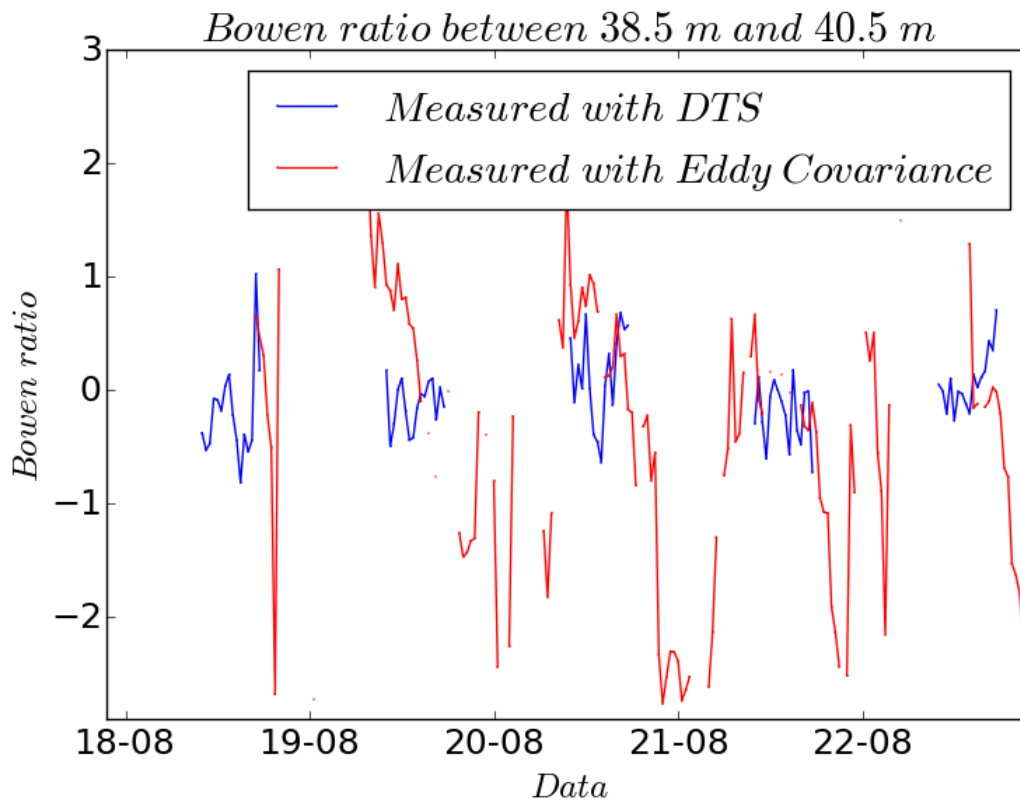
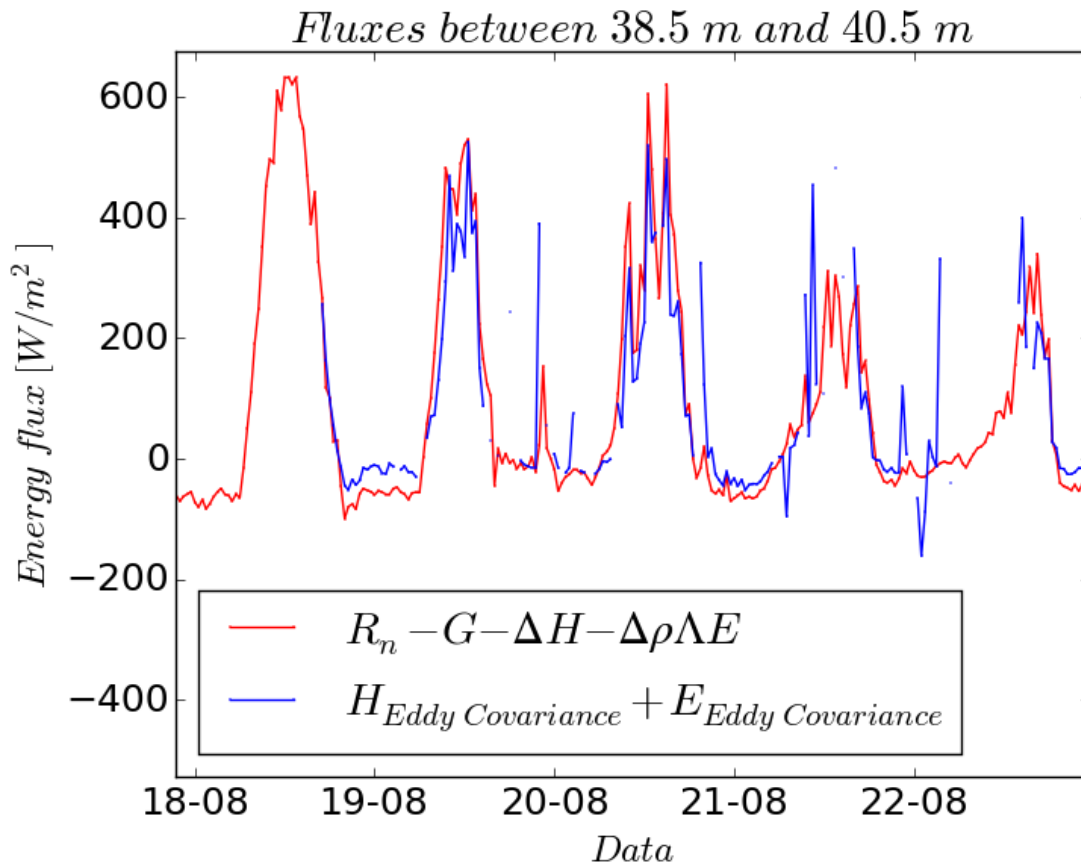




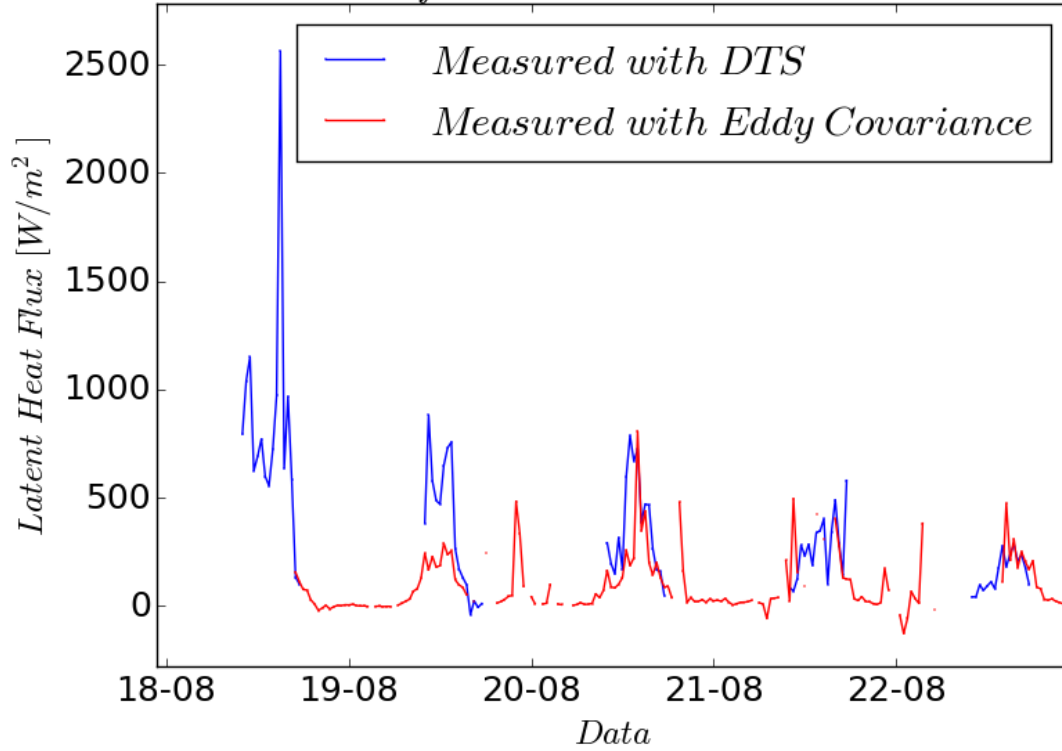








Latent heat fluxes between 38.5 m and 40.5 m



Sensible heat fluxes between 38.5 m and 40.5 m

